

AD 687447

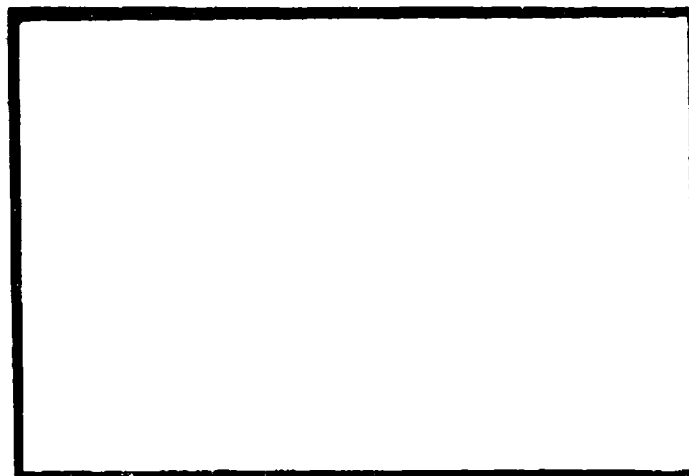
MECHANICAL

TECHNOLOGY

INCORPORATED

U O C  
MAY 27 1969  
RECEIVED

This document has been approved  
for public release and sale; its  
distribution is unlimited.



MECHANICAL TECHNOLOGY INCORPORATED  
968 Albany Shaker Road  
Latham, New York 12110

MTI 69TR23

REFINED SOLUTION OF PNEUMATIC HAMMER  
INSTABILITY OF INHERENTLY COMPENSATED  
HYDROSTATIC THRUST GAS BEARINGS  
by

T. Chiang  
C.H.T. Pan

March 1969

NO. MFI 69TR23

DATE: March 1969

# TECHNICAL REPORT

## REFINED SOLUTION OF PNEUMATIC HAMMER INSTABILITY OF INHERENTLY COMPENSATED HYDROSTATIC THRUST GAS BEARINGS

by  
T. Chiang  
C.H.T. Pan

T. Chiang C.H.T. Pan  
Author (s)

Walter A. Snow  
Approved

\_\_\_\_\_  
Approved

### Prepared under

Contract Nonr-3730(00)

Task NR 062-317/1-9-68

### Prepared for

Department of Defense  
Atomic Energy Commission  
National Aeronautics and Space Administration

### Administered by

Office of Naval Research  
Department of the Navy

Reproduction in Whole or in Part is Permitted  
for any purpose of the U.S. Government

**MTI**  
MECHANICAL TECHNOLOGY INCORPORATED  
**MTI**

948 ALBANY - SHAKER ROAD - LATHAM, NEW YORK - PHONE 785-0922

## TABLE OF CONTENTS

|  | <u>Page No.</u> |
|--|-----------------|
| ABSTRACT .....   | iv              |
| 1. INTRODUCTION .....  | 1               |
| 2. ANALYSIS .....  | 2               |
| 3. LOAD CAPACITY AND DYNAMIC BEARING REACTIONS .....                                     | 15              |
| Steady-State Load Capacity and Stiffness .....   | 15              |
| Dynamic Bearing Reactions .....  | 16              |
| 4. STABILITY .....   | 19              |
| 5. SUMMARY AND CONCLUSIONS .....   | 21              |
| NOMENCLATURE .....   | 22              |
| REFERENCES .....   | 26              |
| APPENDIXES   |                 |
| A - The Matrix Multiplication Method in Solving Ordinary<br>Differential Equations ..... | 27              |
| B - Alternate Method Using the Nozzle Equation .....                                     | 36              |
| FIGURES  |                 |

ABSTRACT

An externally-pressurized gas thrust bearing was analyzed for both static and dynamic characteristics. The bearing is fed through an inherently compensated restrictor into a shallow pocket. The analysis gave special attentions to the significance of the recent finding of restrictor flow (Ref. 4), the trade-off consideration between static stiffness and stability margin, and the effects of the pocket depth.

## 1. INTRODUCTION

Externally pressurized gas bearings have been used in many engineering devices. It is well known that in order for the bearing to have relatively large load capacity and stiffness it is desirable to have recessed pockets immediately after the feeding holes. This causes the externally pressurized gas bearings to be susceptible to pneumatic hammer instability. Analytical investigations on this subject were made in References 1, 2 and 3.

In conventional analyses of externally pressurized bearings, nozzle equations are used in calculating the flow across a restrictor. The dynamic pressure head resulting from expansion through the restrictor is assumed to be completely lost when entering the bearing film. This, however, is not true as reported in References 4 and 5; a measurement of pressure at the restrictor exit indicates that there is considerable pressure recovery. It was shown that the pressure loss coefficient can be correlated with the Reynolds' number (Ref. 4); a linear relationship is chosen for simplicity.

A simple thrust plate with a feeding hole at the center and a recessed pocket immediately after it, is to be analyzed. The same bearing configuration was previously analyzed in Ref. 12 using the above pressure loss coefficient correlation for the restrictor flow and the Reynolds' equation for the bearing film but assuming a uniform pressure in the pocket. This will be modified in the present analysis by writing another Reynolds' equation for the recessed pocket. This modification is particularly significant when the pocket is shallow which is usually the case as the result of a trade-off consideration between stiffness and stability. Perturbation analysis for small oscillation about the equilibrium position will be performed. Based on the perturbation analysis, dynamic bearing stiffness and damping coefficients can be calculated. Using the stability analysis of Ref. 6, stability maps are constructed. The results using the nozzle equation are also presented for comparison.

## 2. ANALYSIS

The configuration of an inherently compensated, hydrostatic, circular, thrust bearing is schematically shown in Fig. 1. Gas at supply pressure  $p_s$  is led through the feeding hole with diameter  $d_f$ , into the recessed pocket before entering the bearing film. For a circular bearing it is convenient to use the polar coordinates. If we further assume circular symmetry, i.e. no misalignment, then the radial coordinate,  $r$ , is the only space variable required to describe the flow and the pressure distribution. In order to facilitate a dynamic analysis let us allow the bearing to have small axial vibrations about its equilibrium position and express the bearing film thickness as

$$h = C + \epsilon \cos \tau \quad (2.1)$$

or in dimensionless form

$$\bar{h} = 1 + \bar{\epsilon} \cos \tau \quad (2.2)$$

where

$$\begin{aligned} \bar{h} &= h/C \\ \bar{\epsilon} &= \epsilon/C \\ C &= \text{equilibrium film thickness} \\ \tau &= \omega t = \text{dimensionless time} \\ \omega &= \text{frequency of vibration} \end{aligned} \quad (2.3)$$

We have assumed that the vibrations are purely sinusoidal. Note that  $\bar{\epsilon}$ , the normalized amplitude of vibration, is a small number.

The well-known time-dependent, isothermal Reynolds' equation can be written in dimensionless form,

$$\frac{1}{\bar{r}} \frac{\partial}{\partial \bar{r}} \left[ (\bar{r}) (\bar{h} + \bar{h}_R)^3 \bar{p} \frac{\partial \bar{p}}{\partial \bar{r}} \right] = \sigma \frac{\partial}{\partial \tau} \left[ \bar{p} (\bar{h} + \bar{h}_R) \right] ; \bar{r}_F < \bar{r} < \bar{r}_R \quad (2.4)$$

$$\frac{1}{\bar{r}} \frac{\partial}{\partial \bar{r}} \left[ \bar{r}^3 \bar{h} \bar{p} \frac{\partial \bar{p}}{\partial \bar{r}} \right] = \sigma \frac{\partial}{\partial \bar{r}} \left[ \bar{p} \bar{h} \right]; \quad \bar{r}_R < \bar{r} < 1 \quad (2.5)$$

where

$$\begin{aligned} \bar{r} &= r/R \\ \bar{p} &= p/p_a \\ \sigma &= \frac{12\mu\omega}{p_a} \left( \frac{R}{C} \right)^2 = \text{squeeze number} \\ \bar{h}_R &= \frac{h_R}{C} = \text{dimensionless depth of recessed pocket} \end{aligned} \quad (2.6)$$

$\bar{r}_F, \bar{r}_R$  = dimensionless radii of the feeding hole and the recessed pocket, see Fig. 1

It is seen that the pressure distributions of both the recessed pocket ( $\bar{r}_F < \bar{r} < \bar{r}_R$ ) and the film ( $\bar{r}_R < \bar{r} < 1$ ) are governed by the respective Reynolds' equations (2.4) and (2.5).

The boundary condition at the outer edge is

$$\bar{p} = 1 \quad \text{at} \quad \bar{r} = 1 \quad (2.7)$$

The pressures at  $\bar{r}_F$  and  $\bar{r}_R$  are designated as follows:

$$\begin{aligned} \text{at } \bar{r} = \bar{r}_F, \quad \bar{p} &= \bar{p}_F \\ \text{at } \bar{r} = \bar{r}_R, \quad \bar{p} &= \bar{p}_E \\ \text{at } \bar{r} = \bar{r}_{R+}, \quad \bar{p} &= \bar{p}_R \end{aligned} \quad (2.8)$$

Note that there is a discontinuity in pressure at  $\bar{r} = \bar{r}_R$ . The pressures,  $\bar{p}_F$ ,  $\bar{p}_E$  and  $\bar{p}_R$ , are yet unknown. Additional pressure flow relationships across the inlet restriction at  $\bar{r} = \bar{r}_F$  and at  $\bar{r} = \bar{r}_R$  are required for the solution. In the literature (Refs. 1, 2, 3) the well-known nozzle formula is used to calculate the expansion of air from  $p_g$  to  $p_F$  and from  $p_E$  to  $p_R$ . If the pressure calculated according to the nozzle equation are accepted, one automatically assumes that the velocity head resulting from expansion through the nozzle is



completely lost. This is not so because part of the velocity head is recovered as indicated by Ref. 4 and 5. In fact, a correlation formula for the pressure drop and the velocity head was obtained by Vohr (Ref. 4). In the following, both methods of approach, the Vohr's correlation formula and the nozzle equation, will be used for the analysis.

#### Using Vohr's Experimental Correlation

The experimental correlation of Vohr (Ref. 4) shows that the pressure drop at the entrance is related to the velocity head by

$$(\Delta p)_{\text{ent}} = K' p_{\text{dyn}} \quad (2.9)$$

where  $p_{\text{dyn}}$  is the dynamic head expressed in the form of a pressure. The film entrance loss coefficient,  $K'$ , is correlated with  $\bar{R}_e$  (or  $\dot{m}/\pi r u$ ) in Ref. 4, which is reproduced in Fig. 2. For all practical purposes, a linear relationship between  $K'$  and  $\bar{R}_e$  is satisfactory. Hence,

$$K' = K \bar{R}_e = K \frac{\dot{m}}{\pi r u} \quad (2.10)$$

Note that  $K$  is a constant, and

$$K = 0.33 \times 10^{-3} \quad (2.11)$$

Applying the above formulation to the restriction at  $\bar{r} = \bar{r}_F$ , we have

$$p_s - p_F = K \cdot \frac{\dot{m}_F}{\pi r_F u} p_{\text{dyn}} \quad (2.12)$$

Here, the velocity head  $p_{\text{dyn}}$  can be obtained by

$$p_{\text{dyn}} = p_s - p_e \quad (2.13)$$

It is to be noted that  $p_e$  is a fictitious pressure through an isentropic expansion which will carry the gas to its downstream Mach numbers corresponding to  $\dot{m}_F$ . This can be realized by noting that

$$\dot{m}_F = \rho_e V_e a_e \quad (2.14)$$

where  $\rho_e$  and  $V_e$  are the density and velocity corresponding to  $p_e$ , and  $a_e$  is the flow cross-sectional area. Observe the following identity

$$\frac{\dot{m}_F}{C^* a_e \rho_s} = \frac{\rho_e}{\rho_s} \frac{V_e}{C^*} = \frac{\rho_e}{\rho_s} M_e^* \quad (2.15)$$

where  $C^*$  = the speed of sound at sonic velocity

$$M_e^* = \frac{V_e}{C^*} = \text{Mach number with respect to } C^* \quad (2.16)$$

Since both  $\rho_e/\rho_s$  and  $M_e^*$  are function of Mach number only (for the fictitious isentropic expansion), let us denote

$$f_e = f(M_e^*) = \frac{\rho_e}{\rho_s} M_e^* \quad (2.17)$$

Then, from Eq. (2.15)

$$\left. \begin{aligned} f_e &= \frac{\dot{m}_F}{C^* a_e \rho_s} = \frac{\rho_e}{\rho_s} M_e^* \\ a_e &= 2\pi r_F (h + h_R) \end{aligned} \right\} \quad (2.18)$$

For a given  $M_e$ , the quantities  $\rho_e/\rho_s$  and  $M_e^*$  can be determined with the aid of a gas table. (Ref. 10). Then  $\dot{m}_F$  can be easily calculated from (2.18). Note that

$$C^* = \sqrt{\frac{2\gamma}{\gamma+1} RT} \quad (2.19)$$

where

$\gamma$  = ratio of specific heats

$R$  = gas constant =  $2.47 \times 10^5 \frac{\text{in}^2}{\text{sec}^2 \cdot R}$  for air

$T$  = absolute temperature of bearing

(2.20)

Conversely, once  $\dot{m}_F$  is known,  $M_e$  can be determined, which in turn yields  $p_e/p_s$ . Similarly, the loss at the second restriction ( $r = r_R$ ) is

$$p - p_R = K \frac{\dot{m}_R}{\pi r_R^4} \quad (2.21)$$

Now,  $p_E$  is obviously the supply pressure for this restrictor and  $p_g$  is the pressure resulting from a fictitious isentropic expansion. Corresponding to (2.18), we have

$$f_g = f(M_g) = \frac{\rho_g}{\rho_e} M_g^* = \frac{\dot{m}_R}{C^* a_g \rho_E} \quad (2.22)$$

$$a_g = 2\pi r_R h$$

In solving the Reynolds' equations (2.4) and (2.5) with small periodic variations of the gap about the equilibrium position, we write in complex form,

$$\bar{h} = 1 + \bar{\epsilon} e^{i\tau} \quad (2.23)$$

and expand the dimensionless pressure

$$\bar{p} = \bar{p}_0 + \bar{\epsilon} \bar{p}_1 e^{i\tau} \quad (2.25)$$

$$\dot{\bar{m}}_F = \dot{\bar{m}}_{F0} + \bar{\epsilon} \dot{\bar{m}}_{F1} e^{i\tau} \quad (2.26)$$

The mass flow rates  $\dot{m}_F$  and  $\dot{m}_R$  can be expressed in terms of pressure gradient as follows:

$$\dot{\bar{m}}_F = -2\pi r_F \frac{(h + h_R)^3}{12\mu} \left[ \rho \frac{\partial p}{\partial r} \right]_{r_F} \quad (2.27)$$

$$\dot{m}_R = -2\pi r_R \frac{h^3}{12\mu} \left[ \rho \frac{\partial p}{\partial r} \right]_{r_R} \quad (2.28)$$

Thus, we have

$$\dot{m}_{Fo} = -\pi \bar{r}_F p_a^2 \frac{(C + h_R)^3}{12\mu RT} \left. \frac{\partial \bar{p}_o^2}{\partial \bar{r}} \right|_{\bar{r}_F} \quad (2.29)$$

$$\dot{m}_{Fl} = \dot{m}_{Fo} \left[ \frac{3}{1 + \bar{h}_R} + 2 \frac{\frac{\partial(\bar{p}_o \bar{p}_l)}{\partial \bar{r}}}{\bar{p}_o^2 / \partial \bar{r}} \right]_{\bar{r}_F} \quad (2.30)$$

and

$$\dot{m}_{Ro} = \pi \bar{r}_R p_a^2 \frac{C^3}{12\mu RT} \left. \frac{\partial \bar{p}_o^2}{\partial \bar{r}} \right|_{\bar{r}_R} \quad (2.31)$$

$$\dot{m}_{Rl} = \dot{m}_{Ro} \left[ 3 + 2 \frac{\frac{\partial(\bar{p}_o \bar{p}_l)}{\partial \bar{r}}}{\bar{p}_o^2 / \partial \bar{r}} \right]_{\bar{r}_R} \quad (2.32)$$

From (2.12) and (2.13) it is clear that

$$\begin{aligned} p_s - p_{Fo} &= \bar{\epsilon} p_{Fl} e^{i\tau} \\ &= K \frac{\dot{m}_{Fo} + \bar{\epsilon} \dot{m}_{Fl} e^{i\tau}}{\pi r_F \mu} \left[ p_s - p_{eo} - \bar{\epsilon} p_{el} e^{i\tau} \right] \end{aligned}$$

Hence,

$$p_s - p_{Fo} = K \frac{\dot{m}_o}{\pi r_F \mu} (p_s - p_{eo}) \quad (2.33)$$

$$-\frac{p_{F1}}{p_s - p_{Fo}} = \frac{\dot{m}_{F1}}{\dot{m}_o} = \frac{p_{e1}}{p_s - p_{eo}} \quad (2.34)$$

Similarly, from (2.21)

$$p_{Eo} - p_{Ro} = K \frac{\dot{m}_{Ro}}{\pi r_R \mu} (p_{Eo} - p_{go}) \quad (2.35)$$

and

$$\frac{p_{E1} - p_{R1}}{p_{Eo} - p_{Ro}} = \frac{\dot{m}_{R1}}{\dot{m}_o} + \frac{p_{E1} - p_{g1}}{p_{Eo} - p_{go}} \quad (2.36)$$

Note that we have already used the steady-state mass conservation relationship.

$$\dot{m}_{Ro} = \dot{m}_{Fo} = \dot{m}_o \quad (2.37)$$

Before we go any further, let us observe that there is a singular point in Eq. (2.4) at  $\bar{r} = 0$ . Although  $\bar{r}$  is never equal to zero ( $\bar{r} > \bar{r}_F > 0$ ), the gradients may become very steep near  $\bar{r} = \bar{r}_F$  if  $\bar{r}_F$  is small in comparison to unity. It is therefore convenient to make the following coordinate transformation.

$$\frac{d\bar{r}}{\bar{r}} = d\xi \quad (2.38)$$

$$\text{or } \ln \bar{r} = \xi \quad (2.39)$$

$$\text{and } \bar{r} \frac{\partial}{\partial \bar{r}} = \frac{\partial}{\partial \xi} \quad (2.40)$$

Under the transformed coordinate, Eqs. (2.4) and (2.5) become

$$\frac{\partial}{\partial \xi} \left[ (\bar{h} + \bar{h}_R)^3 \bar{p} \frac{\partial \bar{p}}{\partial \xi} \right] = e^{2\xi} \sigma \frac{\partial}{\partial \tau} \left[ \bar{p} (\bar{h} + \bar{h}_R) \right] ; \xi_F < \xi < \xi_R \quad (2.41)$$

$$\frac{\partial}{\partial \xi} \left[ \bar{h}^3 \bar{p} \frac{\partial \bar{p}}{\partial \xi} \right] = e^{2\xi} \sigma \frac{\partial}{\partial \tau} (\bar{p} \bar{h}) ; \xi_{R+} < \xi < 0 \quad (2.42)$$

with boundary conditions

$$\left. \begin{array}{ll} \text{at } \xi = \xi_F & \bar{p} = \bar{p}_F \\ \text{at } \xi = \xi_{R-} & \bar{p} = \bar{p}_E \\ \text{at } \xi = \xi_{R+} & \bar{p} = \bar{p}_R \\ \text{at } \xi = 0 & \bar{p} = 1 \end{array} \right\} \quad (2.43)$$

$$\text{where } \xi_F = \ln \bar{r}_F \text{ etc.} \quad (2.44)$$

Applying perturbation to (2.41) and (2.42), we obtain

$$\left. \begin{array}{l} \frac{d}{d\xi} \left[ \frac{d\bar{p}_0}{d\xi} \right]^2 = 0 \\ \frac{\partial}{\partial \xi} \left[ \frac{\partial(\bar{p}_0 \bar{p}_1)}{\partial \xi} \right] = e^{2\xi} \frac{\sigma}{(1+\bar{h}_R)^3} + \left[ \bar{p}_0 + (1+\bar{h}_R) \bar{p}_1 \right] \end{array} \right\} \quad \begin{array}{l} (2.45a) \\ (\xi_F < \xi < \xi_{R-}) \end{array} \quad (2.45b)$$

$$\left. \begin{array}{l} \frac{d}{d\xi} \left[ \frac{d\bar{p}_0}{d\xi} \right]^2 = 0 \\ \frac{\partial}{\partial \xi} \left[ \frac{\partial(\bar{p}_0 \bar{p}_1)}{\partial \xi} \right] = e^{2\xi} \sigma + \left[ \bar{p}_0 + \bar{p}_1 \right] \end{array} \right\} \quad \begin{array}{l} (2.46a) \\ (\xi_{R+} < \xi < 0) \end{array} \quad (2.46b)$$

#### Steady-State Solution

The solutions of Eqs. (2.45a) and (2.46a) satisfying boundary conditions (2.43) are

$$\bar{p}_0 = \left[ \frac{\xi_F \bar{p}_{E0}^2 - \xi_R \bar{p}_{F0}^2}{\xi_F - \xi_R} + \frac{\bar{p}_{F0}^2 - \bar{p}_{E0}^2}{\xi_F - \xi_R} \xi \right]^{1/2} \quad \xi_F < \xi < \xi_{R-} \quad (2.47)$$

$$\bar{p}_o = \left[ 1 + (\bar{p}_{Ro}^2 - 1) \frac{\epsilon}{\epsilon_R} \right]^{1/2} \quad \epsilon_{R+} < \epsilon < 0 \quad (2.48)$$

The quantities  $\bar{p}_{Fo}$ ,  $\bar{p}_{Eo}$  and  $\bar{p}_{Ro}$  are to be determined by mass conservation and pressure drop relationships as follows:

From (2.39) and (2.31)

$$\dot{m}_o = - \frac{1}{2} \frac{(1 + \bar{h}_R)^3}{\Lambda_s^* \bar{p}_s^2} \frac{\bar{p}_{Fo}^2 - \bar{p}_{Eo}^2}{\epsilon_F - \epsilon_R} \quad (2.49)$$

$$\dot{m}_o = - \frac{1}{2} \frac{1}{\Lambda_s^* \bar{p}_s^2} \frac{\bar{p}_{Ro}^2 - 1}{\epsilon_R} \quad (2.50)$$

where  $\dot{m}_o = \frac{\dot{m}_o}{p_s \sqrt{RT} \cdot 2\pi r_F (C + h_R)} = \text{dimensionless mass flux} \quad (2.51)$

$$\Lambda_s^* = \frac{12\mu\sqrt{RT} r_F (C + h_R)}{p_s C^3} = \text{feeding parameter} \quad (2.52)$$

and from (2.33) and (2.35)

$$\bar{p}_s - \bar{p}_{Fo} = K \dot{m}_o \frac{24}{\Lambda_s^*} (1 + \bar{h}_R)^2 \frac{r_F}{C} (\bar{p}_s - \bar{p}_{Eo}) \quad (2.53)$$

$$\bar{p}_{Eo} - \bar{p}_{Ro} = K \dot{m}_o \frac{24}{\Lambda_s^*} (1 + \bar{h}_R)^2 \frac{r_F^2}{C r_R} (\bar{p}_{Eo} - \bar{p}_{go}) \quad (2.54)$$

The dimensionless mass flux has a maximum when the flow is choked. In most circumstances, the choking occurs at the first restrictor because the area is smaller than that of the second restrictor. Then, from Eq. (2.51) we have  $\gamma = 1.4$ ,

$$(\dot{m}_o)_{\text{choked}} = \frac{\rho}{\rho_s} \sqrt{\frac{2\gamma}{\gamma+1}} = 0.68$$

Two additional equations are obtained from Eqs. (2.18) and (2.22),

$$f_e = \dot{m}_o \sqrt{\frac{\gamma-1}{2\gamma}} \quad (2.55)$$

$$f_g = \frac{\bar{p}_s}{\bar{p}_{Eo}} \frac{r_F}{r_R} (1 + \bar{h}_R) \dot{m}_o \sqrt{\frac{\gamma-1}{2\gamma}} \quad (2.56)$$

Recall that  $f_e$  and  $f_g$  are implicit functions of  $\bar{p}_{eo}$  and  $\bar{p}_{go}$  respectively. Thus, we have six equations, (2.49), (2.50), (2.53), (2.54), (2.55) and (2.56) to solve for six unknown quantities,  $\dot{m}_o$ ,  $\bar{p}_{Fo}$ ,  $\bar{p}_{Eo}$ ,  $\bar{p}_{Ro}$ ,  $\bar{p}_{eo}$  and  $\bar{p}_{go}$ . The system is obviously non-linear. Iterative method is used in obtaining the solution.

Numerical computation has been programmed on a computer. Knowing  $\bar{p}_{Fo}$ ,  $\bar{p}_{Eo}$  and  $\bar{p}_{Ro}$ , the steady-state pressure distribution is explicitly given by (2.47) and (2.48).

#### Perturbation Solution

The perturbation pressure is governed by Eqs. (2.45b) and (2.46b) with one obvious boundary condition that  $\bar{p}_1$  must vanish at  $\xi = 0$  ( $\bar{r} = 1$ ). The other boundary conditions are to be derived from the mass conservation and so on as follows:

First of all, since  $\bar{p}_1$  is in general complex, it is convenient to assume

$$\bar{p}_o \bar{p}_1 = u(\xi) + i v(\xi) \quad (2.57)$$

Then, after separating the real and imaginary parts, the differential equations are reduced to

$$\left. \begin{aligned} \frac{d^2 u}{d\xi^2} &= \frac{\sigma}{(1 + \bar{h}_R)^3} e^{2\xi} \left[ \frac{-(1 + \bar{h}_R) v}{\bar{p}_o} \right] \\ \frac{d^2 v}{d\xi^2} &= \frac{\sigma}{(1 + \bar{h}_R)^3} e^{2\xi} \left[ \bar{p}_o + \frac{1 + \bar{h}_R}{\bar{p}_o} u \right] \end{aligned} \right\} \xi_F < \xi < \xi_R \quad (2.58)$$



$$\left. \begin{aligned} \frac{d^2 u}{d\xi^2} &= \sigma e^{2\xi} - \left[ \frac{v}{\bar{p}_0} \right] \\ \frac{d^2 v}{d\xi^2} &= \sigma e^{2\xi} \left[ \bar{p}_0 + \frac{u}{\bar{p}_0} \right] \end{aligned} \right\} \xi_{R+} < \xi < 0 \quad (2.59)$$

Before Eqs. (2.34) and (2.36) can be used as boundary conditions for the differential equations, it is necessary to obtain expressions for  $\bar{p}_{e1}$  and  $\bar{p}_{g1}$ .

Since  $p_e$  and  $f_e$  are functions of  $M_e$  we can write

$$p'_e = \frac{dp_e}{dM_e} M'_e \quad \text{and} \quad f'_e = \frac{df_e}{dM_e} M'_e \quad (2.60)$$

The primed quantities represent perturbations.

Also, from Eq. (2.18)

$$f_e = f_e(\dot{m}_F, a_e) \quad (2.61)$$

Thus,

$$\begin{aligned} f'_e &= \frac{\partial f_e}{\partial \dot{m}_F} \dot{m}'_F + \frac{\partial f_e}{\partial a_e} a'_e \\ &= \frac{f_e}{\dot{m}_{Fo}} \dot{m}'_F - \frac{f_e}{a_e} a'_e \end{aligned} \quad (2.62)$$

Combining (2.60) and (2.62)

$$\bar{p}_{e1} = \frac{d\bar{p}_e}{dM_e} \frac{f_e}{\frac{df_e}{dM_e}} \left[ \frac{\dot{m}'_F}{\dot{m}_{Fo}} - \frac{1}{1 + \bar{h}_R} \right] \quad (2.63)$$

Similarly one can easily obtain

$$\bar{p}_{g1} = \frac{d\bar{p}_g}{dM_g} \frac{f_g}{\frac{df_g}{dM_g}} \left[ \frac{\dot{m}'_R}{\dot{m}_{Ro}} - 1 - \frac{\bar{p}_{E1}}{\bar{p}_{Eo}} \right] \quad (2.64)$$

Using (2.63), (2.64), (2.30) and (2.32), Eqs. (2.34) and (2.36) become

$$\begin{aligned}
 - \frac{1}{\bar{p}_{Fo} (\bar{p}_s - \bar{p}_{Fo})} (u + iv) \Big|_{\xi_F} &= \left( 1 - \frac{H_e}{\bar{p}_s - \bar{p}_{eo}} \right) \left[ 2E^{-1} \frac{\partial(u + iv)}{\partial \xi} \right]_{\xi_F} \\
 + \frac{3}{1 + \bar{h}_R} - \frac{2H_e}{(\bar{p}_s - \bar{p}_{eo})(1 + \bar{h}_R)} & \quad (2.65)
 \end{aligned}$$

$$\begin{aligned}
 \left[ \frac{1}{\bar{p}_{Eo}} \left( \frac{1}{\bar{p}_{Eo} - \bar{p}_{Ro}} \right) - \frac{1}{\bar{p}_{Eo} - \bar{p}_{go}} - \frac{H_g}{\bar{p}_{Eo} - \bar{p}_{go}} \frac{1}{\bar{p}_{Eo}^2} \right] (u + iv) \Big|_{\xi_{R-}} \\
 = \frac{1}{\bar{p}_{Ro} (\bar{p}_{Eo} - \bar{p}_{Ro})} (u + iv) \Big|_{\xi_{R+}} + 2 \left( 1 - \frac{H_g}{\bar{p}_{Eo} - \bar{p}_{go}} \right) \left[ E^{-1} \frac{\partial(u + iv)}{\partial \xi} \right]_{\xi_{R+}} \\
 + 3 - 2 \frac{H_g}{\bar{p}_{Eo} - \bar{p}_{go}} \quad (2.66)
 \end{aligned}$$

where

$$\left. \begin{aligned}
 H_e &= \frac{d\bar{p}_e}{dM_e} f_e / \frac{df_e}{dM_e} \\
 H_g &= \frac{d\bar{p}_g}{dM_g} f_g / \frac{df_g}{dM_g} \\
 E &= \frac{d\bar{p}_o^2}{d\xi}
 \end{aligned} \right] \quad (2.67)$$

$H_e$  and  $H_g$  can be determined by the relationships for an isentropic expansion or by simply using a gas table (Ref. 10).

The mass conservation at  $\xi_R$  yields

$$\frac{3}{1 + \bar{h}_R} + 2 \left[ E^{-1} \frac{\partial(u + iv)}{\partial \xi} \right]_{\xi_{R-}} = 3 + 2 \left[ E^{-1} \frac{\partial(u + iv)}{\partial \xi} \right]_{\xi_{R+}} \quad (2.68)$$

Since the pressure at the exit of the film remains ambient in spite of the gap oscillation, the perturbation pressure must vanish.

$$(u + iv) \Big|_{\xi = 0} = 0 \quad (2.69)$$

Each of the four equations, (2.65), (2.66), (2.68), and (2.69), yields two boundary conditions if their real and imaginary parts are separated. We therefore have eight boundary conditions to solve Eqs. (2.58) and (2.59).

The formulation of the perturbation problem is now complete. The numerical solution of this system is obtained in Appendix A using the matrix multiplication method.

An alternative approach using the nozzle equation instead of Vohr's correlation formula is given in Appendix B.

### 3. LOAD CAPACITY AND DYNAMIC BEARING REACTIONS

The pressure in the feeding hole region ( $r < r_F$ ) is uniform and steady while the pressure distributions in the recessed pocket and in the film are given by

$$\begin{aligned}\bar{p}(\bar{r}, \tau) &= \bar{p}_0(\bar{r}) + \bar{\epsilon} \frac{u + i v}{\bar{p}_0} e^{i\tau} \\ &= \bar{p}_0(\bar{r}) + \bar{\epsilon} \frac{u(\bar{r}) \cos \tau - v(\bar{r}) \sin \tau}{\bar{p}_0(\bar{r})}\end{aligned}\quad (3.1)$$

The bearing force may be obtained by integrating the pressure relative to the ambient, throughout the film. Thus,

$$\begin{aligned}W &= \int_0^R (p - p_a) 2\pi r dr \\ &= \pi r_F^2 (p_s - p_a) + 2\pi \int_{r_F}^R (p - p_a) r dr + 2\pi \int_{r_R}^R (p - p_a) r dr\end{aligned}\quad (3.2)$$

Non-dimensionalizing the load by  $\pi R^2 p_a$ , we have

$$\begin{aligned}\bar{W} = \frac{W}{\pi R^2 p_a} &= \bar{r}_F^2 (\bar{p}_s - 1) + 2 \int_{\bar{r}_F}^{\bar{r}_R} (\bar{p}_0 - 1 + \bar{\epsilon} \bar{p}_1 e^{i\tau}) \bar{r} d\bar{r} \\ &\quad + 2 \int_{\bar{r}_R}^1 (\bar{p}_0 - 1 + \bar{\epsilon} \bar{p}_1 e^{i\tau}) \bar{r} d\bar{r}\end{aligned}\quad (3.3)$$

#### Steady-State Load Capacity and Stiffness

The steady-state load capacity can be obtained by taking the time-independent part of Eq. (3.3).

$$\begin{aligned}\bar{W}_0 &= \bar{r}_F^2 \bar{p}_s - 1 + 2 \int_{\xi_F}^{\xi_R} \bar{p}_0(\xi) e^{2\xi} d\xi \\ &\quad + 2 \int_{\xi_R}^0 \bar{p}_0(\xi) e^{2\xi} d\xi\end{aligned}\quad (3.4)$$

With the steady-state pressure distribution  $\bar{p}_0(\xi)$  solved in the previous section,  $\bar{w}_0$  can be easily obtained by quadrature. The static stiffness is, by definition,

$$\frac{Ck_0}{\pi R^2 p_a} = -C \frac{\partial}{\partial C} (\bar{w}_0) = -\frac{C}{2\Delta C} \left\{ \bar{w}_0^{(+)} - \bar{w}_0^{(-)} \right\} \quad (3.5)$$

where the superscripts (+) and (-) refer to the load capacities at  $C + \Delta C$  and  $C - \Delta C$  respectively.  $\Delta C$  should be sufficiently small; a suitable value for  $\Delta C$  is  $0.01C$ .

### Dynamic Bearing Reaction

The dynamic bearing reaction due to axial vibration is, from the time-dependent part of Eq. (3.3)

$$\begin{aligned} \frac{F_z}{\pi R^2 p_a} &= \bar{e} \cdot 2 \int_{\bar{r}_F}^1 \bar{p}_1 \bar{r} d\bar{r} e^{i\tau} \\ &= \bar{e} R_e \left\{ e^{i\tau} (U_z + i V_z) \right\} \end{aligned} \quad (3.6)$$

where  $U_z$  = Dynamic Stiffness

$$= -2 \int_{\xi_F}^{\xi_R} \frac{u}{\bar{p}_0} e^{2\xi} d\xi - 2 \int_{\xi_R}^0 \frac{u}{\bar{p}_0} e^{2\xi} d\xi \quad (3.7)$$

$V_z$  = Dynamic Damping

$$= -2 \int_{\xi_F}^{\xi_R} \frac{v}{\bar{p}_0} e^{2\xi} d\xi - 2 \int_{\xi_R}^0 \frac{v}{\bar{p}_0} e^{2\xi} d\xi \quad (3.8)$$

Knowing  $u$  and  $v$  from the perturbation solution shown in the previous section, the dynamic stiffness and damping can be readily calculated from Eqs. (3.7) and (3.8) by quadrature.

Numerical computations have been programmed on a computer. Typical results are obtained for a bearing configuration with the following dimensions:

$$\begin{aligned} R &= 2 \text{ in.} \\ r_R &= 0.5 \text{ in.} \\ r_F &= 0.005 \text{ in.} \\ h_R &= 0.002 \text{ in.} \end{aligned}$$

The static stiffness is plotted against  $\Lambda_s^*$  in Figs. 3 and 4 for  $\bar{p}_s = 4$  and 2. It is seen that the static stiffness using Vohr's correlation has a maximum at approximately  $\Lambda_s^* = 0.62$  for  $\bar{p}_s = 4$  and  $\Lambda_s^* = 0.50$  for  $\bar{p}_s = 2$ . The static stiffness using nozzle equation are also plotted for comparison; two different values of the flow discharge coefficient are used, namely,  $C_w = 0.6$  and 1.0. Since  $\Lambda_s^*$  represents the relative importance of the restrictions offered by the restrictor and the bearing film, the peaks of the static stiffness occurs at different  $\Lambda_s^*$  for  $C_w = 0.6$  and 1.0. The flow discharge coefficient for nozzles and orifices was reviewed in Ref. 11. It is reported that  $C_w$  varies from 0.6 to 1.0 depending on flow condition and pressure ratio. In general  $C_w$  is close to 1.0 when the pressure drop across the restrictor is large; this occurs when  $\Lambda_s^*$  is small (large clearance operation). When  $\Lambda_s^*$  is large (small clearance and hence no appreciable pressure drop across the restrictor),  $C_w$  is about 0.6. Although no measurement on  $C_w$  has been made for the inherently compensated restrictor used in this bearing, it is commonly accepted to use values between 0.6 and 1.0. For the bearing configuration under consideration the value of  $C_w = 1.0$  appears to be a good choice as the static stiffness agrees well with that using Vohr's correlation.

Normally, a hydrostatic thrust bearing is designed off the optimum stiffness

point and on the larger  $\Lambda_s^*$  side for more stable operation (See Fig.10) and higher load capacity. It has been observed (Ref.13) that in a hydrostatic journal bearing, the actual stiffness on the high  $\Lambda_s^*$  side is appreciably below the theoretical value (using the nozzle equation and  $C_w = 0.6$ ). The same type of comparison can be expected for hydrostatic thrust bearings. Thus, the present analysis using Vohr's correlation would yield results in better agreement with the actual stiffness.

The stiffness and load capacity for the same bearing except with a larger feeding hole ( $r_F = 0.02$  in. instead of 0.005 in.), are shown in Figs. 5 and 6. The stiffness curves exhibit the same characteristics as the other bearing configuration; it again has a maximum stiffness at  $\Lambda_s^* = 0.60$  if Vohr's correlation is used.

The dynamic stiffness and damping of the bearing with  $r_F = 0.005$  in. are plotted against frequency for various values of  $C$  in Figs. 7 and 8. When the frequency is low ( $\omega \lesssim 1$ ), the dynamic stiffness approaches asymptotically to the value of the static stiffness as can be anticipated. The frequency at which  $V_z = 0$ , is called the critical frequency which will be useful in the stability analysis in the next section.

#### 4. STABILITY

In the previous section, we have calculated the dynamic bearing reactions corresponding to small axial vibrations about the equilibrium (statically) position. These information are directly useful in determining the bearing stability.

In Reference 6, a stability analysis for either a single or two degree-of-freedom system was performed. The results for a single degree-of-freedom system are directly applicable; they may be stated as follows:

Let  $\omega_0$  be the frequency of vibration at which

$$V_z \Big|_{\omega_0} = 0 \quad (4.1)$$

This is the state of neutral stability. Then, the critical mass is given by

$$M_0 = \frac{P_a \pi R^2}{C \omega_0^2} U_z \Big|_{\omega_0} \quad (4.2)$$

A slight variation from the state of neutral stability would cause the system to be unstable if and only if

$$\frac{\partial V_z}{\partial \omega} \Big|_{\omega_0} \delta M > 0 \quad (4.3)$$

where  $\delta M$  is a small mass increment above  $M_0$ . From Figure 8,  $\frac{\partial V_z}{\partial \omega} \Big|_{\omega_0} > 0$ .

Therefore, in order for the bearing to be stable,  $\delta M$  must be less than zero, or, the bearing mass must be kept below the critical mass.

Based on the above and a knowledge of  $U_z$  and  $V_z$ , the critical mass can be calculated from Eq. (4.2). Since Vohr's data (Ref. 4) are essentially for low Mach number flows, only bearings with subsonic flow throughout the passage will



be considered. Supersonic bearings are also currently under investigation.

The critical mass for the bearing with  $R = 2$  in.,  $r_R = 0.5$  in.,  $r_F = 0.005$  in. and  $h_R = 0.002$  in. is plotted against  $\Lambda_s^*$  in Fig. 9 for both methods of calculating restrictor flow. Although the critical mass calculated with  $C_w = 1.0$  still appears to be in closer agreement with that according to Vohr's correlation, its error is not on the conservative side. In Fig. 10, the stiffness and the critical mass using Vohr's correlation are plotted against  $\Lambda_s^*$ . At the point where the stiffness is a maximum, the critical mass is rather low. A trade-off is therefore necessary between the stiffness and the critical mass. Figure 10 then would enable one to decide the design point of a bearing at which a stable operation is possible at the expense of a reasonable decrease in stiffness.

It can also be seen from Fig. 10 that when  $\Lambda_s^*$  is beyond a certain value for a given  $\bar{p}_s$ , the bearing becomes infinitely stable because  $V_z$  is always positive there. Thus, we can obtain a stability map by plotting this critical  $\Lambda_s^*$  against  $\bar{p}_s$  as shown in Fig. 11. Three curves are shown there; the solid one uses Vohr's correlation and the dotted curves use the nozzle formula. Again, the curve with  $C_w = 1.0$  is not conservative. In Fig. 12, stability maps for different values of the pocket-to-film volume ratio are shown. It is seen that the bearing will be more stable for smaller pocket-to-film volume ratio. One can read from Fig. 12 for  $\bar{p}_s = 4$  for example, the values of critical  $\Lambda_s^*$  at different volume ratio.

| $\frac{\pi r_R^2 h_R}{\pi(R^2 - r_R^2)C}$ | $\frac{2}{3}$ | $\frac{1}{3}$ | $\frac{2}{15}$ | $\frac{1}{15}$ |
|---|---------------|---------------|----------------|----------------|
| Critical $\Lambda_s^*$                    | 2.4           | 1.6           | 0.9            | 0.44           |

The dimensionless stiffness and the critical  $\Lambda_s^*$  are plotted against the volume ratio in Fig. 13. Note that we did not show the results with zero volume ratio; the reason was that the flow is choked and supersonic flow in the bearing film would result. From Fig. 13 it is clear that for the geometry chosen there is an optimum volume ratio of approximately 0.1 for maximum dimensionless static stiffness. It should be remarked here that one can design to achieve this stiffness with the assurance that the bearing with  $\Lambda_s^* = 0.7$  (which is the critical value) and volume ratio of 0.1, is at the threshold of absolute stability.

## 5. SUMMARY AND CONCLUSIONS

Inherently compensated hydrostatic bearings with shallow recessed pocket near the feeding hole were analyzed theoretically. Both the bearing film and the recessed pocket are treated by using the isothermal Reynolds' equation. Vohr's correlation for entrance restriction was used to calculate the restrictor flow. Results were compared with those using the nozzle formula instead.

Based on the results obtained, the following conclusions can be drawn:

1. Steady-state load capacity and stiffness were calculated. It was found that the static stiffness has a maximum value when the feeding parameter  $\Lambda_s^*$  is approximately 0.6 for the geometry chosen if Vohr's correlation is used.
2. If the nozzle formula is used to calculate the restrictor flow, then the discharge coefficient  $C_w = 1.0$  yields good results in static stiffness but non-conservative stability margin.
3. Stability results were obtained based on a perturbation analysis which yields dynamic stiffness and dynamic damping. Applying the stability results of Ref. 6, stability maps were constructed. A combined plot of stiffness and critical mass against the feeding parameter shows that it is often necessary to design a bearing off its maximum stiffness in order to gain a sufficient stability margin.
4. The stability margin of a hydrostatic bearing increases with decreasing volume ratio between the recessed pocket and the bearing film.
5. If a hydrostatic bearing is designed at the threshold of absolute stability, there is an optimum pocket-to-film volume ratio at which the static stiffness is a maximum.

# NOMENCLATURE

|                 |   |
|-----------------|---|
| $A_e$           | Area = $2\pi r_F (C + h_R)$                     |
| $C$             | Equilibrium film thickness; Also speed of sound |
| $C^*$           | Speed of sound at sonic speed                   |
| $C_w$           | Nozzle discharge coefficient                    |
| $E$             | Defined in (2.67)                               |
| $\bar{f}(\eta)$ | Defined in (B.3)                                |
| $f_e, f_g$      | Defined in (2.18), (2.22)                       |
| $F_z$           | Dynamic bearing reaction                        |
| $H_e, H_g$      | Defined in (2.67)                               |
| $\bar{H}$       | Matrix defined in (A.20)                        |
| $h$             | Film thickness                                  |
| $h_R$           | Depth of recessed pocket                        |
| $\bar{h}$       | $h/C$ , dimensionless film thickness            |
| $i$             | $\sqrt{-1}$                                     |
| $k_o$           | Static bearing stiffness                        |
| $K'$            | $K \bar{R}_e$                                   |

|                        |   |
|------------------------|---|
| $K$                    | Constant defined in (2.11)                                |
| $M$                    | Mass of bearing   |
| $M_e$                  | Mach number   |
| $M_e^*$                | Mach number based on $C^*$                                |
| $\dot{m}$              | Mass flow rate  |
| $\dot{m}_0$            | Steady-state mass flow rate                               |
| $\bar{m}$              | Dimensionless mass flow rate, Eq. (2.51)                  |
| $p$                    | Pressure  |
| $p_a$                  | Ambient pressure  |
| $p_{dyn}$              | Dynamic pressure head                                     |
| $p_e$                  | Defined in (2.13)   |
| $p_g$                  | Defined in (2.21)   |
| $p_s$                  | Supply pressure   |
| $\bar{p}$              | $p/p_s$   |
| $\bar{p}_0, \bar{p}_1$ | Steady-state and perturbation pressure, defined in (2.24) |
| $r$                    | Radial coordinate   |
| $\bar{r}$              | $r/R$   |

|               |  |
|---------------|--|
| $r_F$         | Radius of feeding hole                   |
| $r_R$         | Radius of recessed pocket                |
| $R$           | Bearing radius                           |
| $\bar{R}_e$   | Reynold's number = $\dot{m}/(\pi r \mu)$ |
| $R$           | Gas constant                             |
| $T$           | Temperature                              |
| $t$           | Time                                     |
| $U_z$         | Dimensionless dynamic stiffness          |
| $V_z$         | Dimensionless dynamic damping            |
| $u, v$        | Defined in (2.57)                        |
| $V$           | Gas velocity                             |
| $W$           | Bearing load capacity                    |
| $\bar{W}$     | $W/\pi R^2 p_a$                          |
| $\gamma$      | Ratio of specific heats                  |
| $e$           | Amplitude of axial vibration             |
| $\bar{e}$     | Dimensionless $e$ , $\bar{e} = e/C$      |
| $\Lambda_s^*$ | Feeding parameter, defined in (2.52)     |

|            |                                  |
|------------|----------------------------------|
| $\mu$      | Viscosity                        |
| $\xi$      | $\ln \bar{r}$                    |
| $\rho$     | Density                          |
| $\sigma$   | Squeeze number, defined in (2.6) |
| $\tau$     | Dimensionless time, $\omega t$   |
| $\omega$   | Frequency of vibration           |
| $\omega_0$ | Critical $\omega$                |

#### Subscript

|        |  |
|--------|--|
| $0, 1$ | Steady-state and perturbation quantities       |
| F,E,R  | Pertaining to geometrical location, see Fig. 1 |

#### Superscripts

|   |                                  |
|---|----------------------------------|
| - | Denotes dimensionless quantities |
| k | Indicates station                |

# REFERENCES

1. Licht, L., Fuller, D.D., and Sternlicht, B., "Self-Excited Vibration of an Air-Lubricated Thrust Bearing," Trans. ASME, vol. 80, p.411, 1958.
2. Licht, L., and Elrod, H.G., Jr., "An Analytical and Experimental Study of the Stability of Externally Pressurized, Gas-Lubricated Thrust Bearings," The Franklin Institute, Report No. 1-A2049-12, 1961.
3. Lund, J., Wernick, R.J., and Malanoski, S.B., "Analysis of the Hydrostatic Journal and Thrust Gas Bearing for the NASA AB-5 Gyro Gimbal Bearing," MTI Technical Report 62TR26, 1962.
4. Vohr, J., "An Experimental Study of Flow Phenomena in the Feeding Region of an Externally Pressurized Gas Bearing," MTI Technical Report 65TR47, 1966.
5. Carfagno, S.P., and McCabe, J.T., "Summary of Investigations of Entrance Effects in Circular Thrust Bearings," Franklin Institute Research Laboratories Interim Report 1-A2049, 1965.
6. Pan, C.H.T., "Spectral Analysis of Gas Bearing Systems for Stability Studies," presented at the Ninth Midwestern Mechanics Conference, University of Wisconsin, Madison, Wis., August, 1965.
7. Ralston, A., and Wilf, H.S., "Mathematical Methods for Digital Computers," John Wiley & Sons, Inc., New York, N.Y., 1960.
8. Castelli, V., and Pirvics, J., "Equilibrium Characteristics of Axial-Groove Gas Lubricated Bearings," ASLE-ASME-ASLE Lubrication Conference, San Francisco, California, October, 1965.
9. Hildebrand, F.B., "Introduction to Numerical Analysis," McGraw-Hill Co., New York, N.Y., 1956.
10. Keenan, J.H. and Kaye, J., "Gas Tables" John Wiley & Sons, Inc., 1956.
11. Hsing, F.C. and Chiang, T., "A Review of the Discharge Coefficient of Orifices and Nozzles," MTI-65-TM7, October, 1965.
12. Chiang, T., and Pan, C.H.T., "Analysis of Pneumatic Hammer Instability of Inherently Compensated Hydrostatic Thrust Gas Bearings" MTI-66TR47, January 1967.
13. Wilson, D., Private Communication on his unpublished experimental data.

# APPENDIX A THE MATRIX MULTIPLICATION METHOD IN SOLVING ORDINARY DIFFERENTIAL EQUATIONS

The differential equations (2.58) and (2.59) derived in Section 2 are to be solved by using the matrix multiplication method. Rewrite the equation in the following form.

$$\left. \begin{aligned} u'' + f_1 v &= f_2 \\ v'' + g_1 u &= g_2 \end{aligned} \right\} \quad \xi_F < \xi < \xi_R \quad (A.1)$$

$$\left. \begin{aligned} u'' + \bar{f}_1 v &= \bar{f}_2 \\ v'' + \bar{g}_1 u &= \bar{g}_2 \end{aligned} \right\} \quad \xi_{R+} < \xi < 0 \quad (A.2)$$

where

$$\left. \begin{aligned} f_1 &= \frac{\sigma}{(1 + \bar{h}_R)^2} \frac{e^{2\xi}}{\bar{p}_0} = -g_1 \\ f_2 &= 0 \\ g_2 &= \frac{\sigma}{(1 + \bar{h}_R)^3} e^{2\xi} \bar{p}_0 \\ \bar{f}_1 &= \sigma e^{2\xi} \bar{p}_0 = -\bar{g}_1 \\ \bar{f}_2 &= 0 \\ g_2 &= \sigma e^{2\xi} \bar{p}_0 \end{aligned} \right\} \quad (A.3)$$

The primes represent derivations with respect to  $\xi$ . If we divide the distance between  $\xi_F$  and  $\xi_R$  into  $N$  equal intervals and the distance between  $\xi_R$  and 0 into  $Q$  intervals,

$$\begin{aligned} \Delta_1 &= \frac{\xi_R - \xi_F}{N} \\ \Delta_2 &= \frac{0 - \xi_R}{Q} \end{aligned} \quad (A.4)$$



then, in central difference form,

$$\left. \begin{aligned} u'(g_k) &= \frac{u^{k+1} - 2u^k + u^{k-1}}{\Delta_1} \\ u''(g_k) &= \frac{u^{k+1} - 2u^k + u^{k-1}}{\Delta_1^2} \end{aligned} \right\} \quad k = 0, 1, 2, \dots, N$$

$$\left. \begin{aligned} u'(g_k) &= \frac{u^{k+1} - 2u^k + u^{k-1}}{\Delta_2} \\ u''(g_k) &= \frac{u^{k+1} - 2u^k + u^{k-1}}{\Delta_2^2} \end{aligned} \right\} \quad k = N', N+1, \dots, N+Q$$

where  $u^k = u(g_k)$ . Note that stations  $N$  and  $N'$  occupy the same physical location.

Substitute into Eqs. (A.1) and (A.2) and write the results in matrix form

$$\begin{bmatrix} A^k \end{bmatrix} y^{k+1} + \begin{bmatrix} B^k \end{bmatrix} y^k + \begin{bmatrix} C^k \end{bmatrix} y^{k-1} = d^k, \quad (k = 0, 1, 2, \dots, N) \quad (A.5)$$

$$\begin{bmatrix} \bar{A}^k \end{bmatrix} y^{k+1} + \begin{bmatrix} \bar{B}^k \end{bmatrix} y^k + \begin{bmatrix} \bar{C}^k \end{bmatrix} y^{k-1} = \bar{d}^k, \quad (k = N', N+1, \dots, N+Q) \quad (A.6)$$

where

$$A^k = \frac{1}{\Delta_1^2} [I] = \frac{1}{\Delta_1^2} \begin{bmatrix} 1 & 0 \\ 0 & 1 \end{bmatrix}$$

$$B^k = \begin{bmatrix} \frac{-2}{\Delta_1^2} & f_1^k \\ g_1^k & \frac{-2}{\Delta_1^2} \end{bmatrix}$$

$$C^k = A^k$$

$$d^k = \begin{bmatrix} f_2^k \\ g_2^k \end{bmatrix} ; \quad y^k = \begin{bmatrix} u^k \\ v^k \end{bmatrix}$$

$$\bar{A}^k = \frac{1}{\Delta_1^2} [I]$$

$$\bar{B}^k = \begin{bmatrix} \frac{-2}{\Delta_2^2} & \bar{f}_1^k \\ \bar{g}_1^k & \frac{-2}{\Delta_2^2} \end{bmatrix}$$

$$\bar{C}^k = \bar{A}^k$$

$$\bar{d}^k = \begin{bmatrix} \bar{f}_2^k \\ \bar{g}_2^k \end{bmatrix}$$

Assume that the y-vector at station "k+1" can be expressed by

$$y^{k+1} = M^k y^k + m^k \quad (A.7)$$

Here,  $M^k$  and  $m^k$  are unknown matrix and vector at station "k". Combining (A.6) and (A.7) we obtain

$$\begin{bmatrix} M^{k-1} = \left[ \bar{A}^k M^k + \bar{B}^k \right]^{-1} \left[ -\bar{C}^k \right] \\ m^{k-1} = \left[ \bar{A}^k M^k + \bar{B}^k \right]^{-1} (\bar{d}^k - \bar{A}^k m^k) \end{bmatrix} \quad k = N', N+1, \dots, N+Q \quad (A.8)$$

From boundary condition (2.69) it is obvious that

$$y^{N+Q} = \begin{bmatrix} 0 \\ 0 \end{bmatrix} \quad (A.9)$$

Using (A.7) and setting  $k = N + Q - 1$ ,

$$y^{N+Q} = M^{N+Q-1} y^{N+Q-1} + m^{N+Q-1} \quad (A.10)$$

Since  $y^{N+Q-1}$  is not equal to zero, in order to satisfy (A.9) we must have

$$\begin{aligned} M^{N+Q-1} &= 0 \\ m^{N+Q-1} &= 0 \end{aligned} \quad (A.11)$$

Using (A.8) as the recursion formula, the following is easily obtained.

$$\begin{aligned} M^{N+Q-2} &= \left[ \frac{1}{A^{N+Q-1}} M^{N+Q-1} + \frac{1}{B^{N+Q-1}} \right]^{-1} \left[ -\frac{1}{C^{N+Q-1}} \right] \\ m^{N+Q-2} &= \left[ \frac{1}{A^{N+Q-1}} M^{N+Q-1} + \frac{1}{B^{N+Q-1}} \right]^{-1} \left( \frac{1}{d^{N+Q-1}} - \frac{1}{A^{N+Q-1}} m^{N+Q-1} \right) \\ M^{N+Q-3} &= \left[ \frac{1}{A^{N+Q-2}} M^{N+Q-2} + \frac{1}{B^{N+Q-2}} \right]^{-1} \left[ -\frac{1}{C^{N+Q-2}} \right] \\ m^{N+Q-3} &= \left[ \frac{1}{A^{N+Q-2}} M^{N+Q-2} + \frac{1}{B^{N+Q-2}} \right]^{-1} \left( \frac{1}{d^{N+Q-2}} - \frac{1}{A^{N+Q-2}} m^{N+Q-2} \right) \end{aligned} \quad (A.12)$$

$$\begin{aligned} M^{N'} &= \left[ \frac{1}{A^{N+1}} M^{N+1} + \frac{1}{B^{N+1}} \right]^{-1} \left[ -\frac{1}{C^{N+1}} \right] \\ m^{N'} &= \left[ \frac{1}{A^{N+1}} M^{N+1} + \frac{1}{B^{N+1}} \right]^{-1} \left( \frac{1}{d^{N+1}} - \frac{1}{A^{N+1}} m^{N+1} \right) \end{aligned}$$

Define

$$\begin{aligned} \alpha_1 &= \frac{1}{\bar{p}_{E0}} (\bar{p}_{R0} - \bar{p}_{g0}) - H_g \frac{\bar{p}_{E0} - \bar{p}_{R0}}{\bar{p}_{E0}^2} \\ \alpha_2 &= (\bar{p}_{E0} - \bar{p}_{g0}) / \bar{p}_{R0} \\ \alpha_3 &= 2\xi_R (\bar{p}_{E0} - \bar{p}_{g0} - H_g) (\bar{p}_{E0} - \bar{p}_{R0}) / (\bar{p}_{R0}^2 - 1) \\ \alpha_4 &= \left[ 3 (\bar{p}_{E0} - \bar{p}_{g0}) - 2H_g \right] (\bar{p}_{E0} - \bar{p}_{R0}) \end{aligned} \quad (A.13)$$

Then, Eq. (2.66) takes the form,

$$\alpha_1 (u + iv) \Big|_{\xi_{R-}} = \alpha_2 (u + iv) \Big|_{\xi_{R+}} + \alpha_3 \frac{\partial (u + iv)}{\partial \xi} \Big|_{\xi_{R+}} + \alpha_4$$

or,

$$\alpha_1 y^N = \alpha_2 y^{N'} + \frac{\alpha_3}{\Delta_2} \left( -\frac{1}{2} y^{N+2} + 2y^{N+1} - \frac{3}{2} y^{N'} \right) + C_4 \quad (A.14)$$

where  $C_4 = \begin{bmatrix} \alpha_4 \\ 0 \end{bmatrix}$ . We have used the forward difference formula.

From (A.7), one can write

$$y^{N+2} = M^{N+1} y^{N+1} + m^{N+1}$$

$$y^{N+1} = M^{N'} y^{N'} + m^{N'}$$

Substituting into (A.14) results in

$$\alpha_1 y^N = \begin{bmatrix} G \end{bmatrix} y^{N'} + g \quad (A.15)$$

where

$$\begin{bmatrix} G \\ g \end{bmatrix} = \begin{bmatrix} \left( \alpha_2 - \frac{3}{2} \frac{\alpha_3}{\Delta_2} \right) I \\ -\frac{1}{2} \frac{\alpha_3}{\Delta_2} m^{N+1} + \frac{\alpha_3}{\Delta_2} \left( -\frac{1}{2} M^{N+1} + 2I \right) m^{N'} + C_4 \end{bmatrix} \quad (A.16)$$

From (2.68) we have

$$\frac{\partial (u + iv)}{\partial \xi} \Big|_{\xi_{R-}} = \alpha_5 \frac{\partial (u + iv)}{\partial \xi} \Big|_{\xi_{R+}} + \alpha_6 \quad (A.17)$$

$$\text{where } \left. \begin{aligned} \alpha_5 &= \frac{\bar{p}_{Fo}^2 - \bar{p}_{Eo}^2}{\bar{\epsilon}_F - \bar{\epsilon}_R} \frac{\bar{\epsilon}_R}{\bar{p}_{Ro}^2 - 1} \\ \alpha_6 &= \frac{\bar{p}_{Fo}^2 - \bar{p}_{Eo}^2}{\bar{\epsilon}_F - \bar{\epsilon}_R} \frac{3}{2} \frac{\bar{h}_R}{1 + \bar{h}_R} \end{aligned} \right] \quad (\text{A.18})$$

Thus,

$$\left[ \frac{3}{2} y^N - 2 y^{N-1} + \frac{1}{2} y^{N-2} \right] = \frac{\Delta_1 \alpha_5}{\Delta_2} \left[ -\frac{1}{2} y^{N+2} + 2 y^{N+1} - \frac{3}{2} y^{N'} \right] + \begin{bmatrix} \Delta_1 \alpha_6 \\ 0 \end{bmatrix}$$

Using (A.5) to eliminate  $y^{N-2}$ , and (A.7) to eliminate  $y^{N+2}$  and  $y^{N+1}$ , we obtain

$$\begin{aligned} & \left[ \frac{3}{2} I - \frac{1}{2} [C^{N-1}]^{-1} [A^{N-1}] \right] y^N + \left[ -2I - \frac{1}{2} [C^{N-1}]^{-1} [B^{N-1}] \right] y^{N-1} + \frac{1}{2} [C^{N-1}]^{-1} d^{N-1} \\ &= \frac{\Delta_1}{\Delta_2} \alpha_5 \left\{ [\bar{H}] y^{N'} + \left[ -\frac{1}{2} M^{N+1} + 2I \right] m^{N'} - \frac{1}{2} m^{N+1} \right\} + C_6 \end{aligned} \quad (\text{A.19})$$

where

$$\left. \begin{aligned} [\bar{H}] &= \left[ -\frac{1}{2} M^{N+1} + 2I \right] \left[ M^{N'} \right] - \frac{3}{2} I \\ C_6 &= \begin{bmatrix} \Delta_1 \alpha_6 \\ 0 \end{bmatrix} \end{aligned} \right] \quad (\text{A.20})$$

Using (A.15) to eliminate  $y^{N'}$  in (A.19),

$$\begin{aligned} [L] y^N &= \left[ 2I + \frac{1}{2} [C^{N-1}]^{-1} [B^{N-1}] \right] y^{N-1} + \left\{ -\frac{1}{2} [C^{N-1}]^{-1} d^{N-1} + C_6 \right. \\ &\quad \left. + \frac{\Delta_1}{\Delta_2} \alpha_5 [\bar{H} G^{-1} g + \left[ -\frac{1}{2} M^{N+1} + 2I \right] m^{N'} - \frac{1}{2} m^{N+1}] \right\} \end{aligned} \quad (\text{A.21})$$

where

$$[L] = \frac{3}{2} I - \frac{1}{2} [C^{N-1}]^{-1} [A^{N-1}] - \frac{\Delta_1}{\Delta_2} \alpha_1 \alpha_5 \bar{H} G^{-1} \quad (A.22)$$

Thus, by comparing (A.7) with (A.21) it is clear that

$$M^{N-1} = 2 [L]^{-1} + \frac{1}{2} [L]^{-1} [C^{N-1}]^{-1} [B^{N-1}] \quad (A.23)$$

$$\begin{aligned} m^{N-1} = & - \frac{1}{2} [L]^{-1} [C^{N-1}]^{-1} d^{N-1} + [L]^{-1} c_6 \\ & + \frac{\Delta_1}{\Delta_2} \alpha_5 \left( [L]^{-1} [\bar{H}] [G]^{-1} g + [L]^{-1} \left[ -\frac{1}{2} M^{N+1} + 2 I \right] m^{N'} - \frac{1}{2} [L]^{-1} m^{N+1} \right) \end{aligned} \quad (A.24)$$

From which we can calculate the rest of the M's and m's.

$$\left. \begin{aligned} M^{N-2} &= \left[ A^{N-1} M^{N-1} + B^{N-1} \right]^{-1} \left[ -C^{N-1} \right] \\ m^{N-2} &= \left[ A^{N-1} M^{N-1} + B^{N-1} \right]^{-1} \left[ d^{N-1} - A^{N-1} m^{N-1} \right] \\ M^{N-3} &= \left[ A^{N-2} M^{N-2} + B^{N-2} \right]^{-1} \left[ -C^{N-2} \right] \\ m^{N-3} &= \left[ A^{N-2} M^{N-2} + B^{N-2} \right]^{-1} \left[ d^{N-2} - A^{N-2} m^{N-2} \right] \end{aligned} \right\} \quad (A.25)$$

Finally, from boundary condition (2.65),

$$\begin{aligned} - \frac{1}{\bar{p}_{Fo} (\bar{p}_s - \bar{p}_{Fo})} y^{(0)} = & \left( 1 - \frac{H_e/p_a}{\bar{p}_s - \bar{p}_{eo}} \right) 2 \frac{\bar{e}_F - \bar{e}_R}{\bar{p}_{Fo} - \bar{p}_{Lo}} \frac{1}{\Delta_1} \left( -\frac{1}{2} y^{(2)} + 2y^{(1)} - \frac{3}{2} y^{(0)} \right) \\ & + \frac{3}{1 + \bar{h}_R} - \frac{2 H_e/p_a}{(\bar{p}_s - \bar{p}_{eo}) (1 + \bar{h}_R)} \end{aligned} \quad (A.26)$$

Define

$$\left. \begin{aligned} \alpha_7 &= \frac{1}{\bar{p}_{Fo}(\bar{p}_s - \bar{p}_{Fo})} \\ \alpha_8 &= \left(1 - \frac{H_e/p_a}{\bar{p}_s - \bar{p}_{eo}}\right)^2 \frac{\bar{e}_F - \bar{e}_R}{\bar{p}_{Fo} - \bar{p}_{eo}} \\ \alpha_9 &= \frac{3}{1 + \bar{h}_R} - \frac{2 H_e/p_a}{(\bar{p}_s - \bar{p}_{eo})(1 + \bar{h}_R)} \end{aligned} \right] \quad (A.27)$$

Then, Eq. (A.26) becomes

$$\begin{aligned} &\left[ \left( \alpha_7 - \frac{3}{2} \frac{\alpha_8}{\Delta_1} \right) I - \frac{1}{2} \frac{\alpha_8}{\Delta_1} M^{(1)} M^{(o)} + 2 \frac{\alpha_8}{\Delta_1} M^{(o)} \right] y^{(o)} \\ &+ \frac{\alpha_8}{\Delta_1} \left[ -\frac{1}{2} M^{(1)} + 2 I \right] m^{(o)} - \frac{\alpha_8}{2\Delta_1} m^{(1)} + c_9 = 0 \end{aligned} \quad (A.28)$$

where

$$c_9 = \begin{bmatrix} \alpha_9 \\ 0 \end{bmatrix}$$

Thus,

$$\begin{aligned} y^{(o)} &= - \left[ \left( \alpha_7 - \frac{3}{2} \frac{\alpha_8}{\Delta_1} \right) I - \frac{1}{2} \frac{\alpha_8}{\Delta_1} M^{(1)} M^{(o)} + 2 \frac{\alpha_8}{\Delta_1} M^{(o)} \right]^{-1} \\ &\quad \left( \frac{\alpha_8}{\Delta_1} \left[ -\frac{1}{2} M^{(1)} + 2 I \right] m^{(o)} - \frac{\alpha_8}{2\Delta_1} m^{(1)} + c_9 \right) \end{aligned} \quad (A.29)$$

Knowing  $y^{(0)}$  from (A.29) and  $M$ 's and  $m$ 's from (A.12) and (A.25), we can write down the solution as follows:

$$\begin{aligned}
 y^{(1)} &= M^{(0)} y^{(0)} + m^{(0)} \\
 y^{(2)} &= M^{(1)} y^{(1)} + m^{(1)} \\
 &\vdots \\
 y^N &= M^{N-1} y^{N-1} + m^{N-1} \\
 y^{N'} &= \alpha_1 [G]^{-1} y^N - [G]^{-1} g \\
 y^{N+1} &= M^{N'} y^{N'} + m^{N'} \\
 y^{N+2} &= M^{N+1} y^{N+1} + m^{N+1} \\
 &\vdots \\
 y^{N+Q} &= M^{N+Q-1} y^{N+Q-1} + m^{N+Q-1}
 \end{aligned} \tag{A.30}$$



# APPENDIX B ALTERNATE METHOD USING THE NOZZLE EQUATION

Instead of using the Vohr's correlation formula, the well-known nozzle equation will be used to compute the flow and pressure drop through the restrictors. The mass flow rates at  $r_F$  and  $r_R$  are

$$\dot{m}_F = C_w [2\pi r_F (h + h_R)] \sqrt{\frac{2\gamma}{\gamma-1}} \frac{p_s}{\sqrt{RT}} \bar{f} \left( \frac{p}{p_s} \right) \quad (B.1)$$

$$\dot{m}_R = C_w (2\pi r_R h) \sqrt{\frac{2\gamma}{\gamma-1}} \frac{p_E}{\sqrt{RT}} \bar{f} \left( \frac{p}{p_E} \right) \quad (B.2)$$

where  $C_w$  = discharge coefficient

$$\bar{f}(\eta) \equiv \eta^{\frac{1}{\gamma}} \left[ 1 - \eta^{\frac{\gamma-1}{\gamma}} \right]^{1/2} \quad (B.3)$$

Nondimensionalize the mass flux by

$$\rho_s \sqrt{RT} 2\pi r_F (C + h_R) \text{ as before,}$$

$$\dot{\bar{m}}_F = C_w \sqrt{\frac{2\gamma}{\gamma-1}} \left( 1 + \frac{1}{1 + \bar{h}_R} \bar{\epsilon} e^{i\tau} \right) \bar{f} \left( \frac{p}{p_s} \right) \quad (B.4)$$

$$\dot{\bar{m}}_R = C_w \sqrt{\frac{2\gamma}{\gamma-1}} \frac{1}{1 + \bar{h}_R} (1 + \bar{\epsilon} e^{i\tau}) \frac{r_R}{r_F} \frac{p_E}{p_s} \bar{f} \left( \frac{p}{p_E} \right) \quad (B.5)$$

Apply perturbation to (B.4) and (B.5)

$$\begin{aligned} \dot{\bar{m}}_{F0} + \bar{\epsilon} \dot{\bar{m}}_{F1} e^{i\tau} &= C_w \sqrt{\frac{2\gamma}{\gamma-1}} \left( 1 + \frac{1}{1 + \bar{h}_R} \bar{\epsilon} e^{i\tau} \right) \\ &\quad \left( \bar{f} \left| \frac{p_{F0}}{p_s} \right. + \frac{d\bar{f}}{d\eta} \left| \frac{p_{F0}}{p_s} \right. \bar{\epsilon} \frac{p_{F1}}{p_s} e^{i\tau} \right) \end{aligned} \quad (B.6)$$

$$\begin{aligned} \bar{m}_{Ro} + \bar{\epsilon} \bar{m}_{R1} e^{i\tau} &= C_w \sqrt{\frac{2\gamma}{\gamma-1}} \frac{1 + \bar{\epsilon} e^{i\tau}}{1 + \bar{h}_R} \frac{\bar{r}_R}{\bar{r}_F} \frac{\bar{p}_{Eo} + \bar{\epsilon} \bar{p}_{E1} e^{i\tau}}{\bar{p}_s} \\ \left\{ \bar{f} \left| \frac{\bar{p}_{Ro}}{\bar{p}_{Eo}} + \frac{d\bar{f}}{d\eta} \right| \frac{\bar{p}_{Ro}}{\bar{p}_{Eo}} \left( \frac{1}{\bar{p}_{Eo}} \bar{\epsilon} \bar{p}_{R1} e^{i\tau} - \frac{\bar{p}_{Ro}}{\bar{p}_{Eo}^2} \bar{\epsilon} \bar{p}_{E1} e^{i\tau} \right) \right\} \end{aligned} \quad (B.7)$$

Thus, we have

$$\bar{m}_o = C_w \sqrt{\frac{2\gamma}{\gamma-1}} \bar{f} \left| \frac{\bar{p}_{Fo}}{\bar{p}_s} \right| \quad (B.8)$$

$$\bar{m}_o = C_w \sqrt{\frac{2\gamma}{\gamma-1}} \frac{1}{1 + \bar{h}_R} \frac{\bar{r}_R}{\bar{r}_F} \frac{\bar{p}_{Fo}}{\bar{p}_s} \bar{f} \left| \frac{\bar{p}_{Ro}}{\bar{p}_{Eo}} \right| \quad (B.9)$$

Equations (B.8), (B.9), (2.49) and (2.50) can be solved for  $\bar{m}_o$ ,  $\bar{p}_{Fo}$ ,  $\bar{p}_{Eo}$  and  $\bar{p}_{Ro}$ . Hence, the steady-state pressure distribution is readily obtained by Eqs. (2.47) and (2.48).

The differential equations derived for the perturbation pressure are of course still applicable in this method. Equations (B.6) and (B.7) should be used to obtain boundary conditions to replace Eqs. (2.65) and (2.66).

From Eqs. (2.30) and (B.6), we obtain, after some manipulation,

$$\frac{1}{\bar{p}_s \bar{p}_{Fo}} (u + iv) \left| \frac{\bar{f}}{\bar{r}_F} \right| = \frac{\bar{f}}{\frac{d\bar{f}}{d\eta}} \left| \frac{\bar{p}_{Fo}}{\bar{p}_s} \right| \left\{ \frac{2}{1 + \bar{h}_R} + 2 \left[ E^{-1} \frac{\partial(u + iv)}{\partial \xi} \right] \right\} \quad (B.10)$$

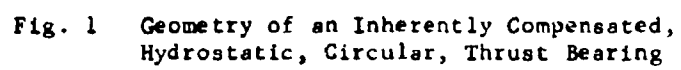
Similarly, from Eqs. (2.32) and (B.7)

$$\left( \frac{1}{\bar{p}_{Eo}^2} - \frac{d\bar{f}/d\eta}{\bar{f}} \right) \left| \frac{\bar{p}_{Ro}}{\bar{p}_{Eo}} \right| \frac{\bar{p}_{Ro}}{\bar{p}_{Eo}^3} (u + iv) \Big|_{\xi_{R-}} + \frac{d\bar{f}/d\eta}{\bar{f}} \left| \frac{\bar{p}_{Ro}}{\bar{p}_{Eo}} \right| \frac{1}{\bar{p}_{Ro} \bar{p}_{Eo}} (u + iv) \Big|_{\xi_{R+}} \\ = 2 + 2 \left[ E^{-1} \frac{\partial(u + iv)}{\partial \xi} \right] \Big|_{\xi_{R+}} \quad (B.11)$$

Comparing (B.10), (B.11) with (2.65), (2.66), it can be seen that if we define

$$\alpha'_1 = \frac{1}{\bar{p}_{Eo}^2} - \mathcal{L} \left| \frac{\bar{p}_{Ro}}{\bar{p}_{Eo}} \right| \frac{\bar{p}_{Ro}}{\bar{p}_{Eo}^3} \\ \alpha'_2 = -\mathcal{L} \left| \frac{\bar{p}_{Ro}}{\bar{p}_{Eo}} \right| \frac{1}{\bar{p}_{Ro} \bar{p}_{Eo}} \\ \alpha'_3 = \frac{2\xi_R}{\bar{p}_{Ro}^2 - 1} \\ \alpha'_4 = 2 ; \mathcal{L} \equiv \frac{d\bar{f}/d\eta}{\bar{f}} \\ \alpha'_7 = - \frac{1}{\bar{p}_s \bar{p}_{Fo}} \\ \alpha'_8 = \frac{1}{\mathcal{L} \left| \frac{\bar{p}_{Fo}}{\bar{p}_s} \right|} 2 \frac{\xi_F - \xi_R}{\bar{p}_{Fo}^2 - \bar{p}_{Eo}^2} \\ \alpha'_9 = \frac{1}{\mathcal{L} \left| \frac{\bar{p}_{Fo}}{\bar{p}_s} \right|} \frac{2}{1 + \bar{h}_R} \quad (B.12)$$

the numerical scheme in Appendix A can be used for this alternative method utilizing the nozzle equation provided that  $\alpha_1$ ,  $\alpha_2$ , etc. are replaced by the primed quantities defined in (B.12).



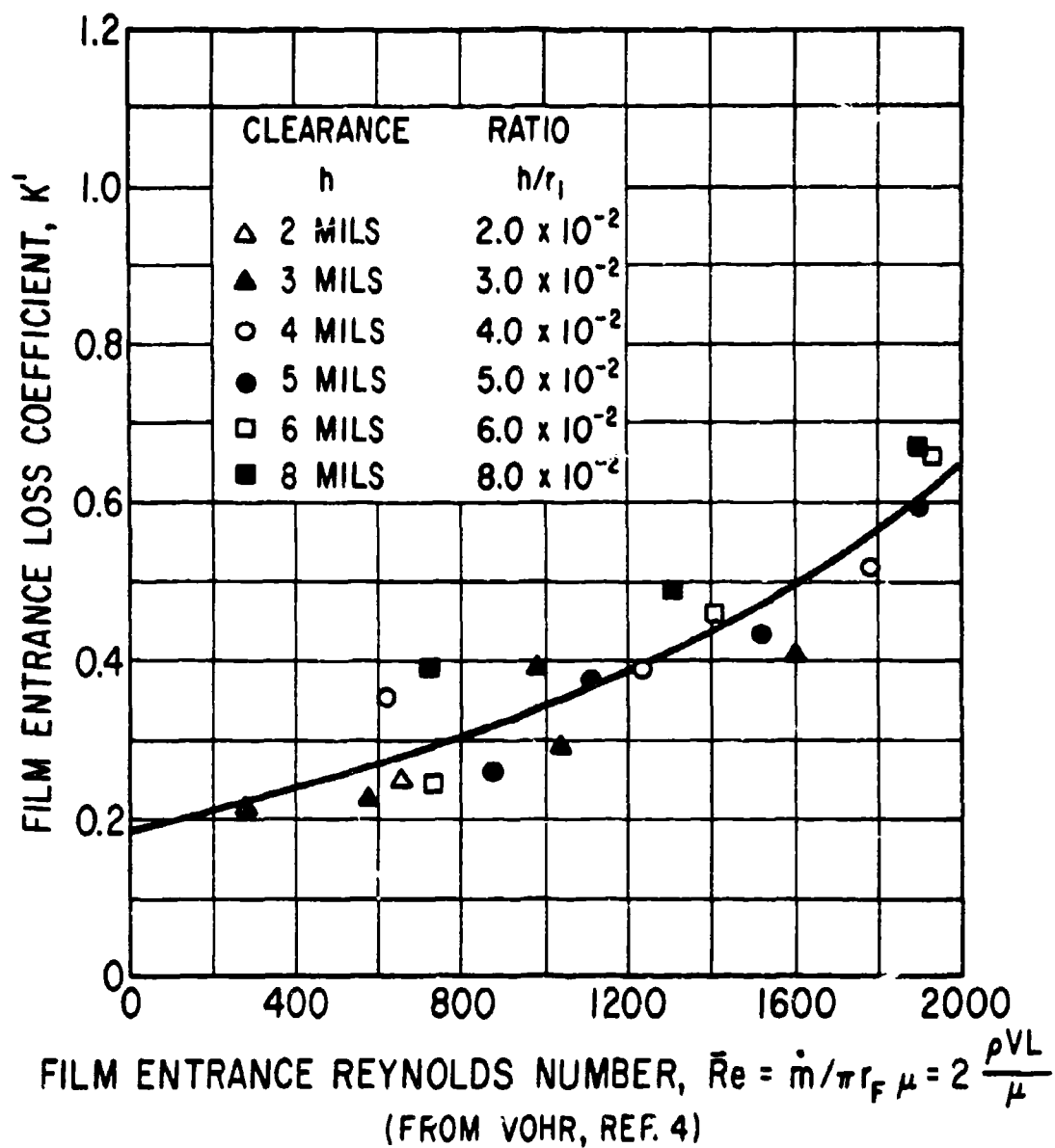


Fig. 2 Loss Coefficient versus Film Entrance Reynolds Number

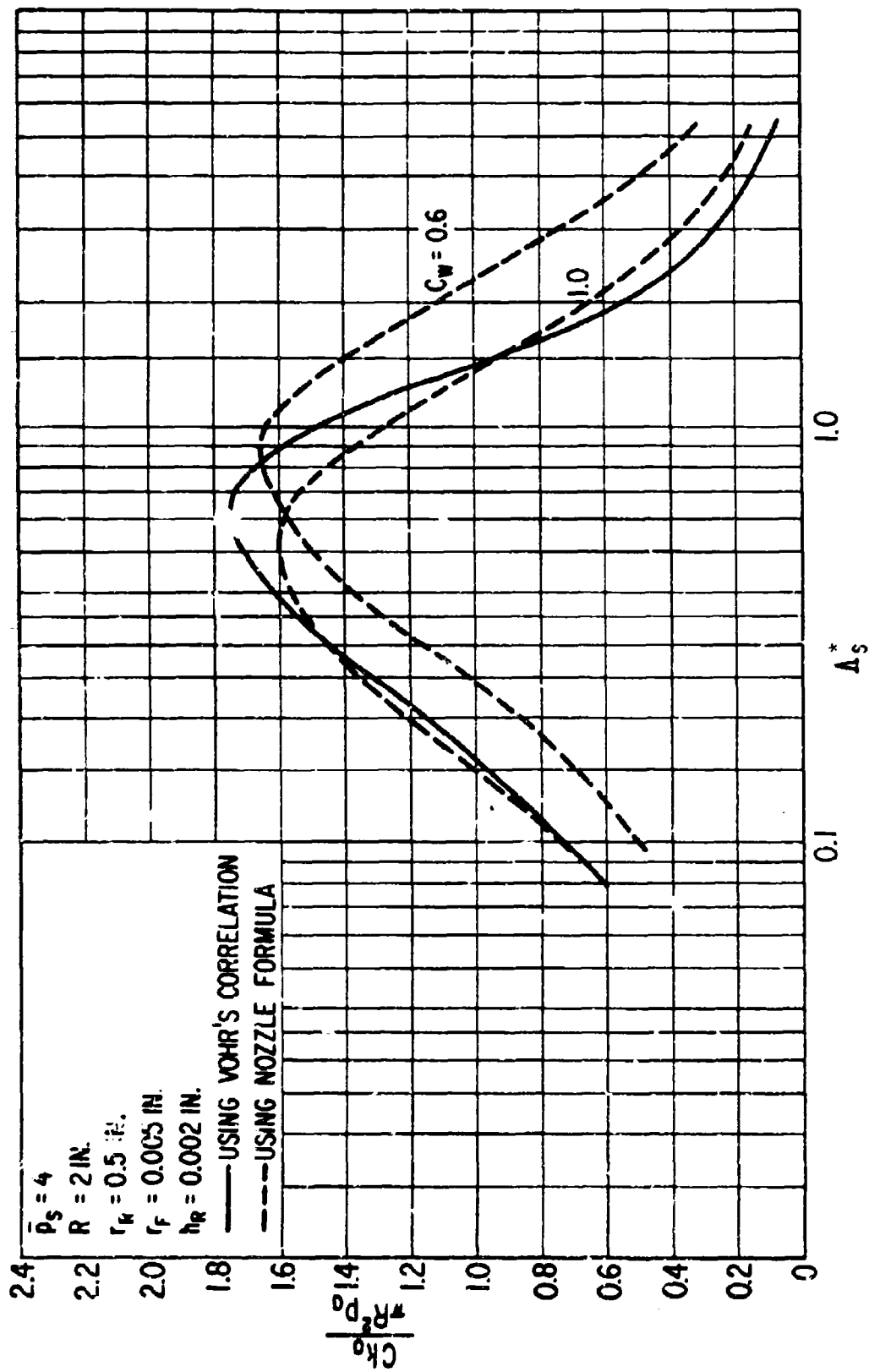


FIG. 3 Static Stiffness versus  $A_s^*$  at  $\bar{p}_s = 4$

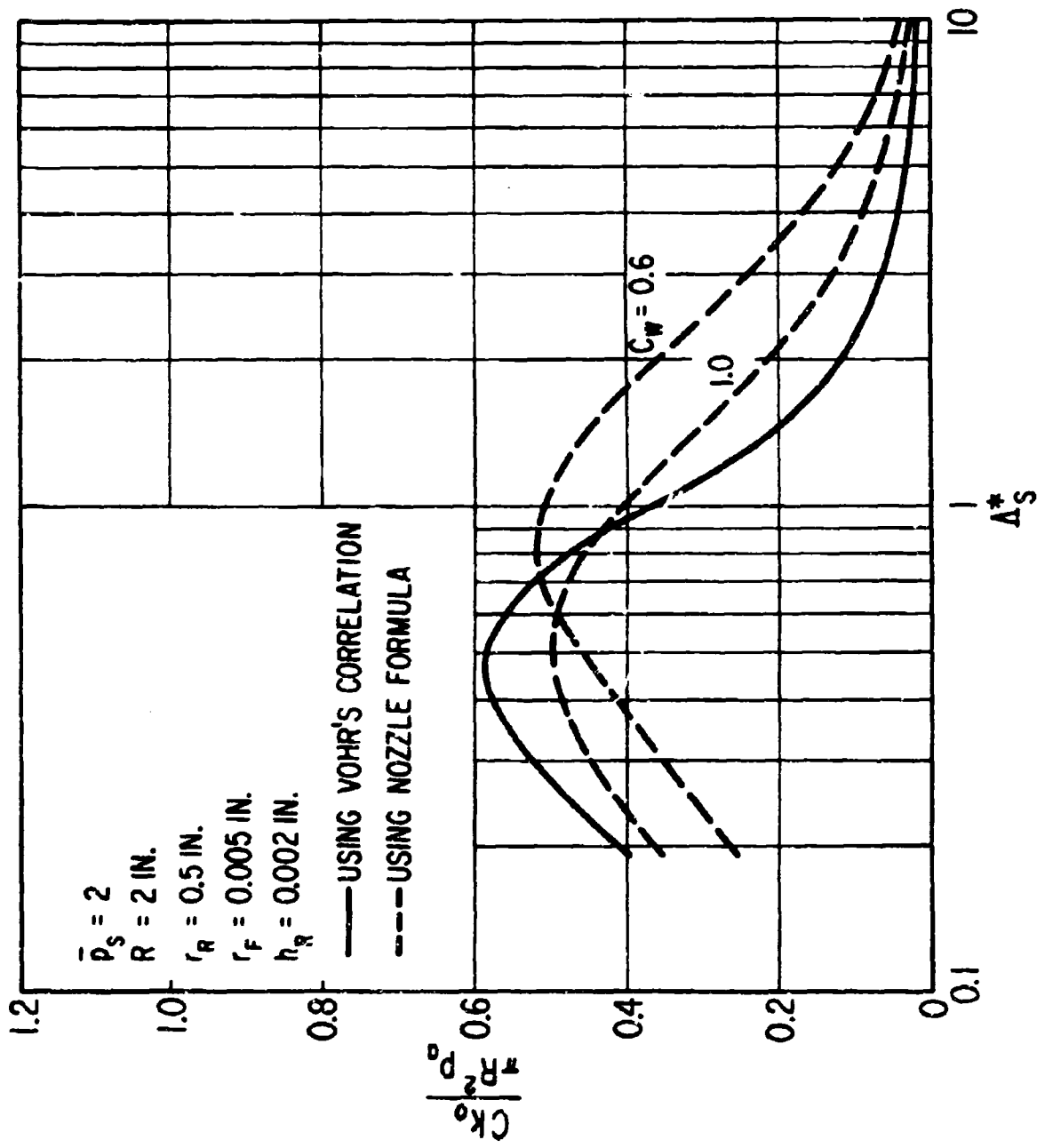


Fig. 4 Static Stiffness versus  $\Lambda_s^*$  at  $\bar{P}_g = 2$



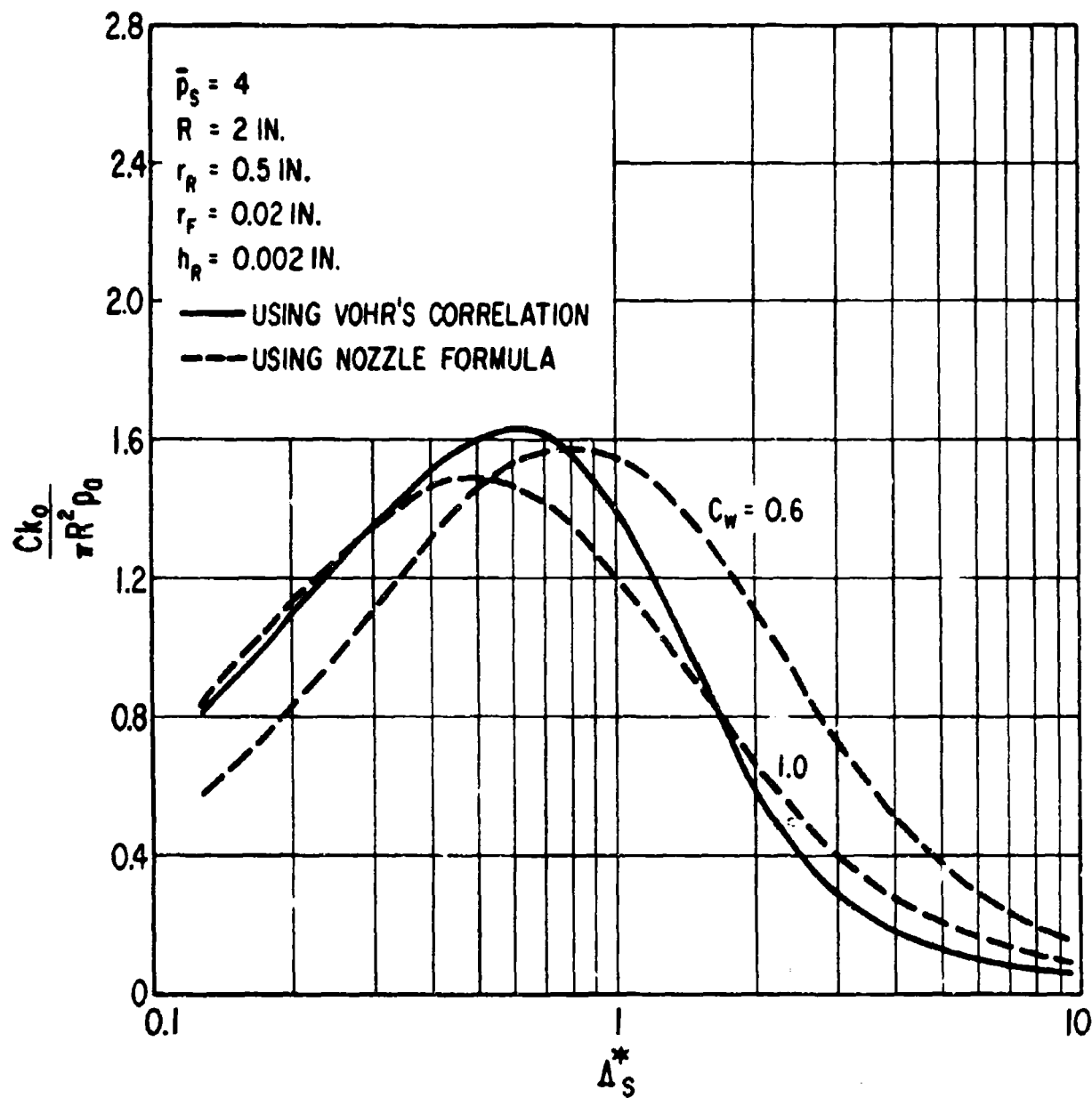


Fig. 5 Static Stiffness versus  $\Lambda_S^*$  with  $r_F = 0.02 \text{ in.}$

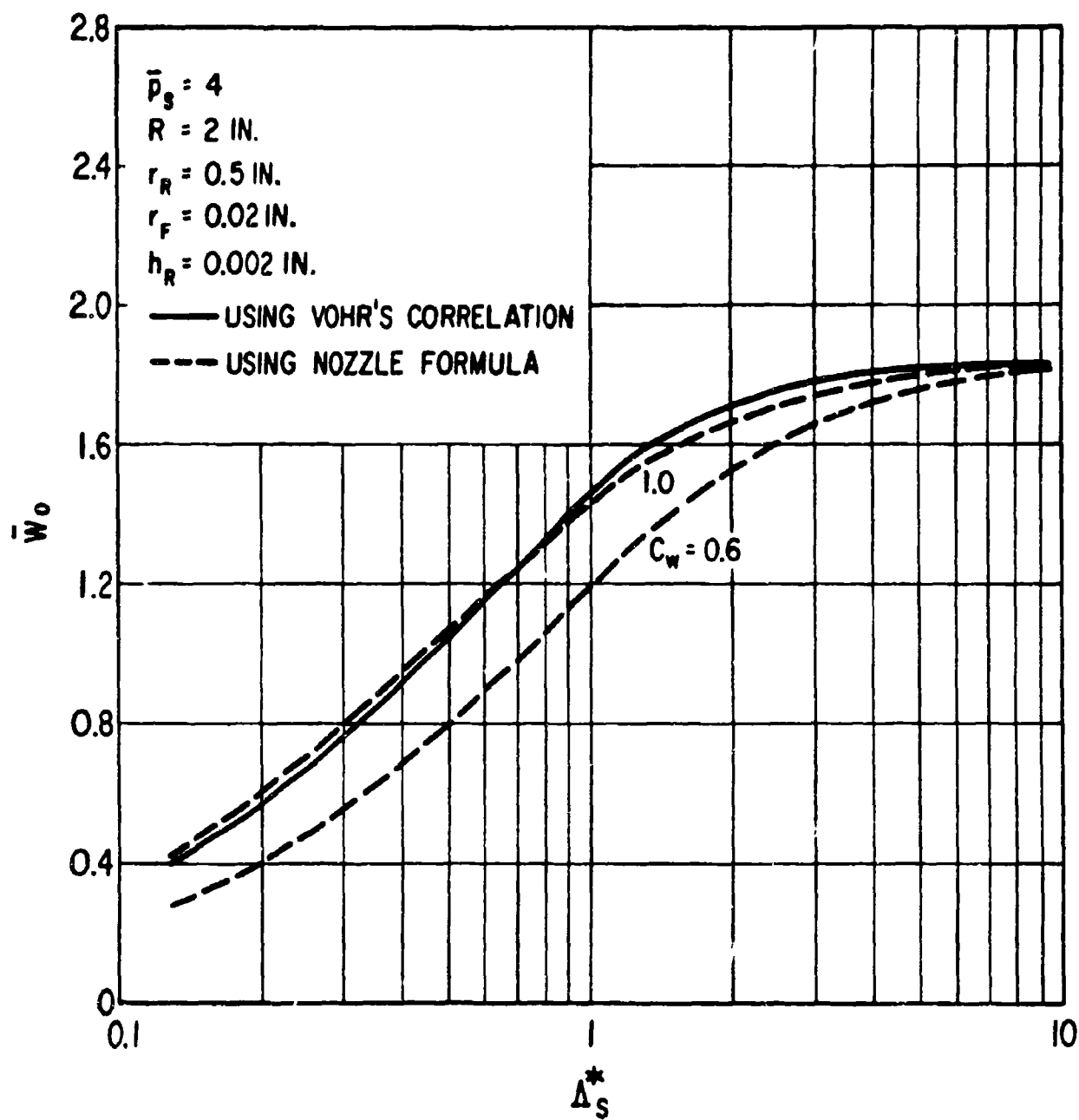


Fig. 6 Load Capacity versus  $\Delta S^*$

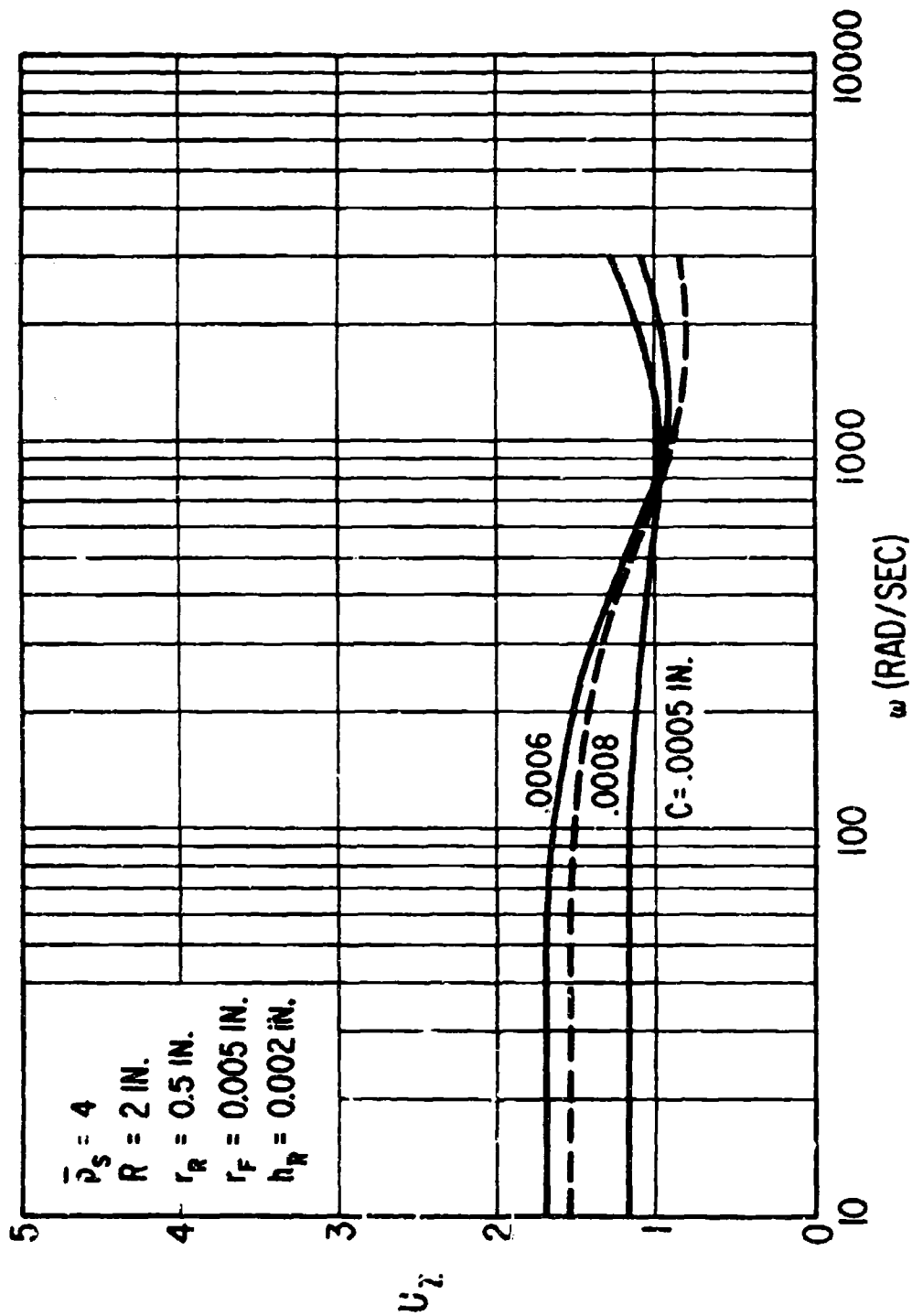


Fig. 7 Dynamic Stiffness  $U_z$  versus Frequency  $\omega$

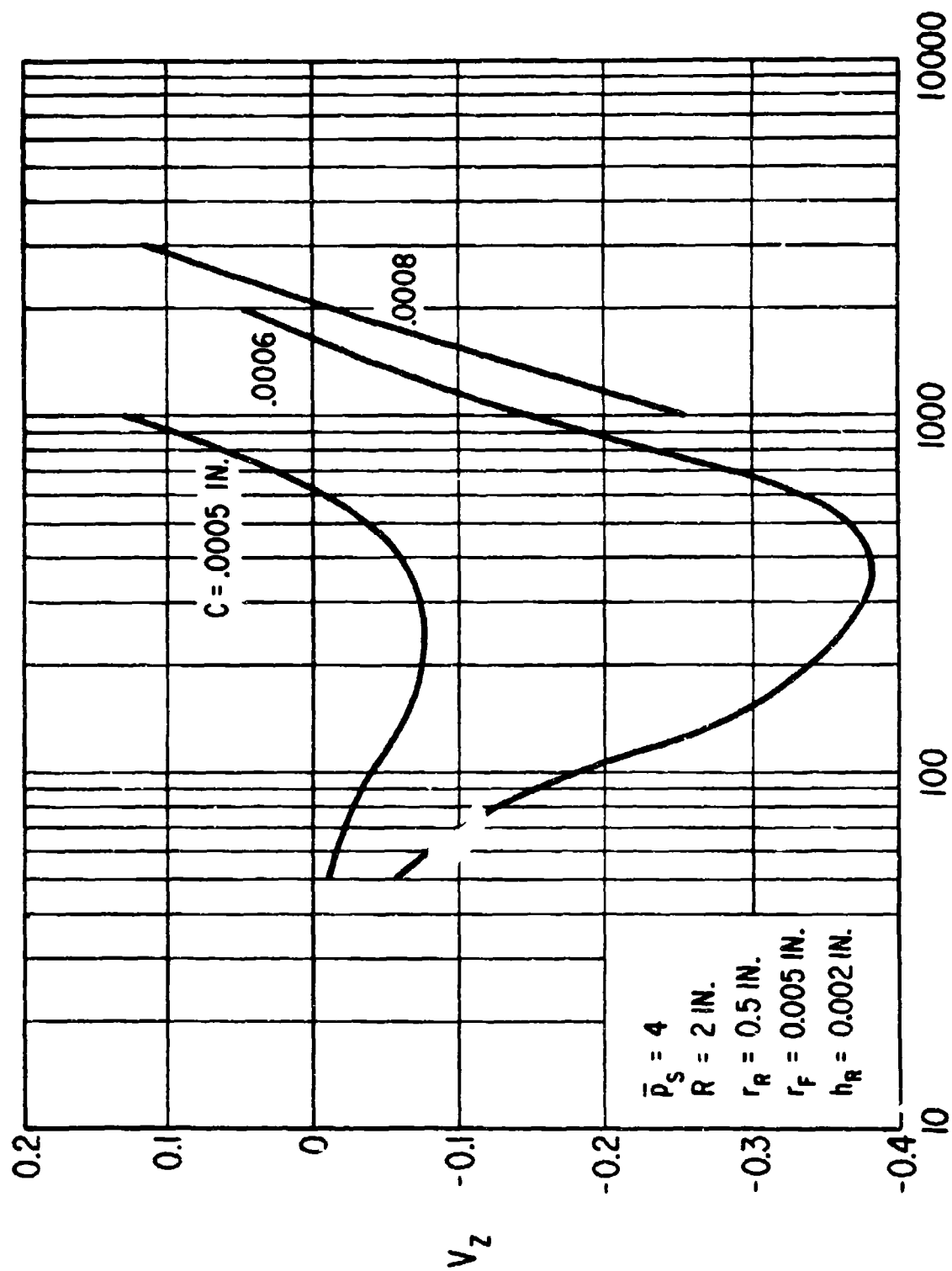


Fig. 8 Dynamic Damping  $V_z$  versus Frequency  $\omega$

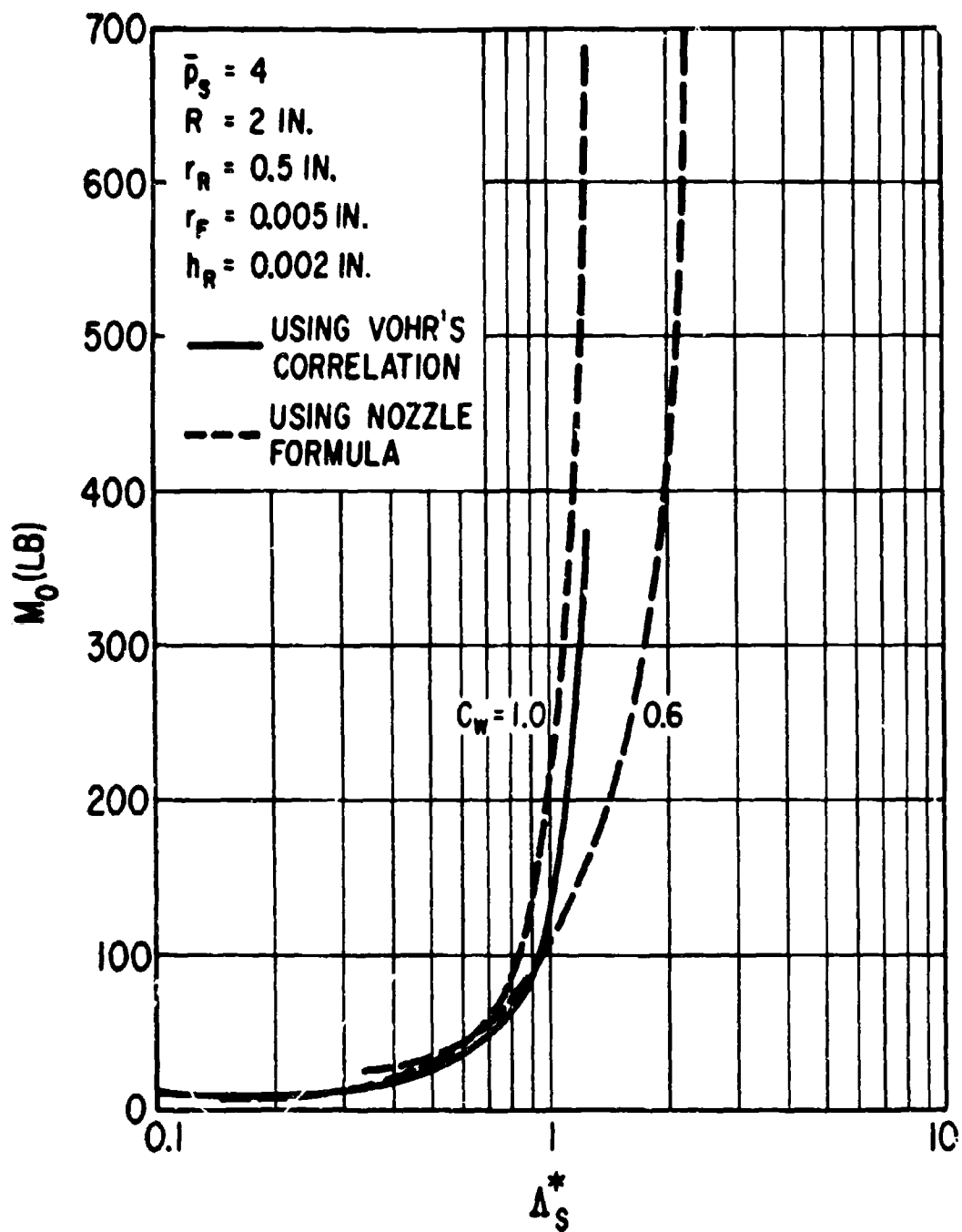


Fig. 9. Critical Mass versus  $\Delta_s^*$

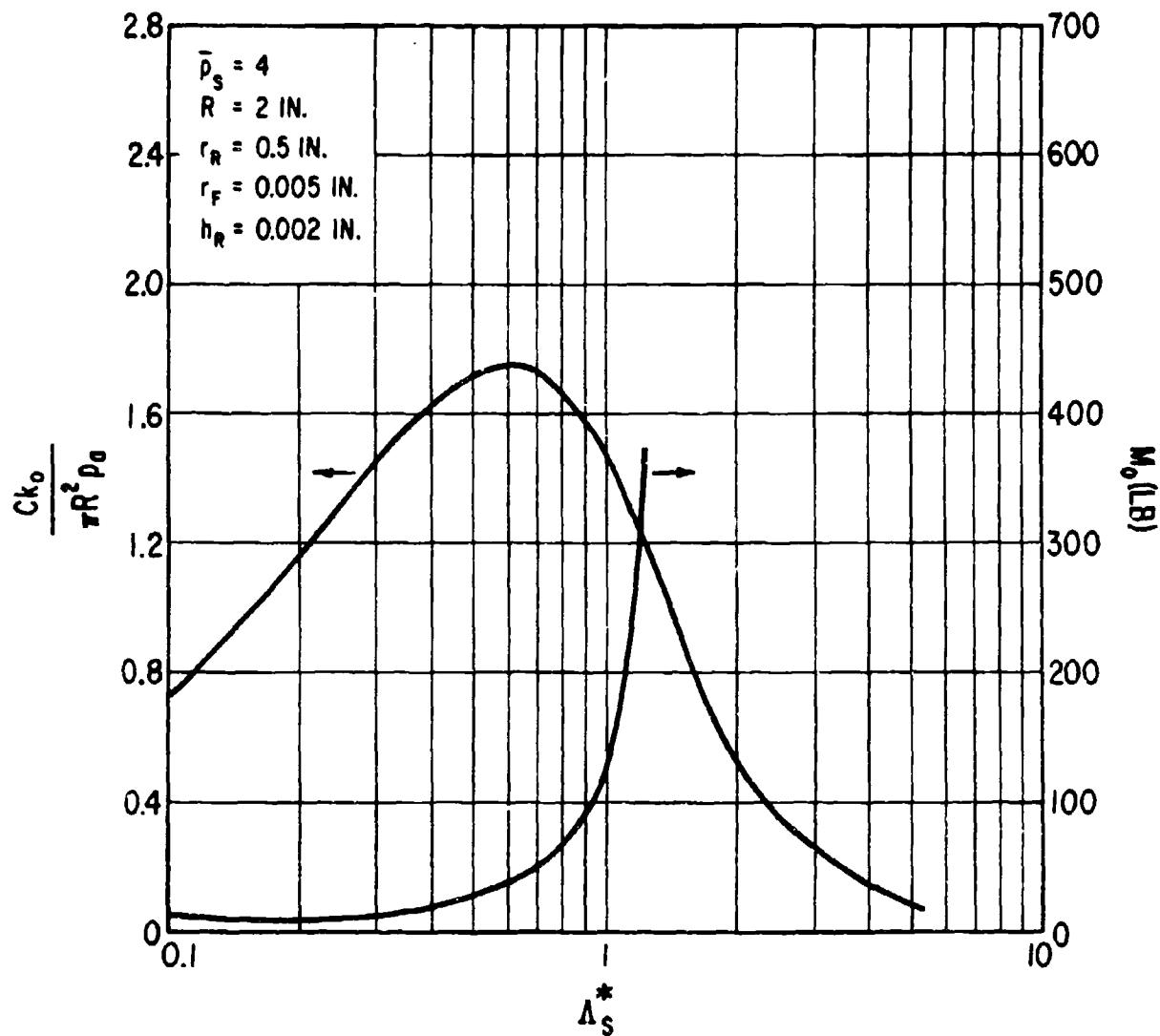


Fig. 10 Critical Mass and Static Stiffness versus  $\Lambda_S^*$  using Vohr's Correlation

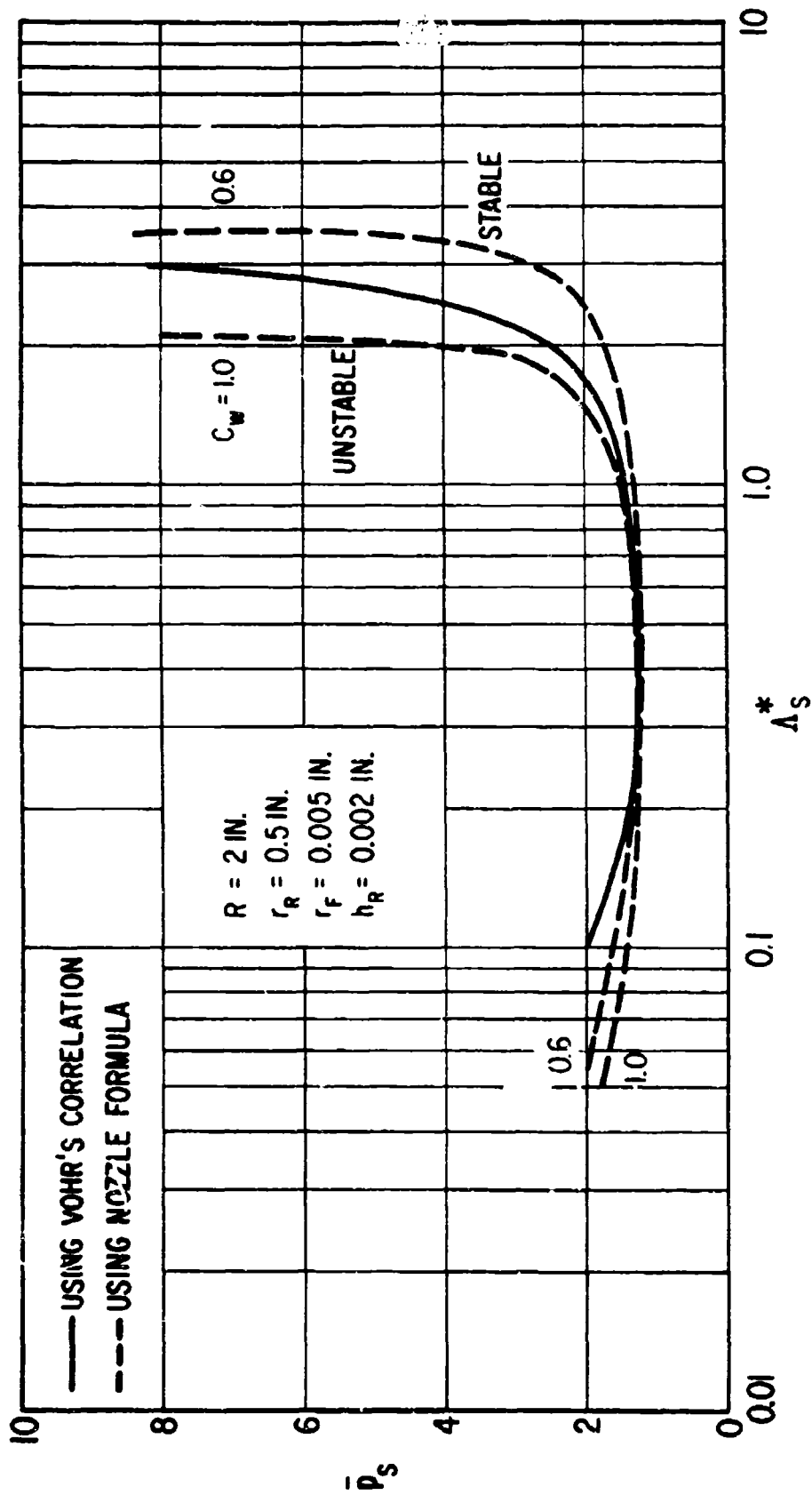


Fig. 11 Stability Map at a Fixed Pocket Depth

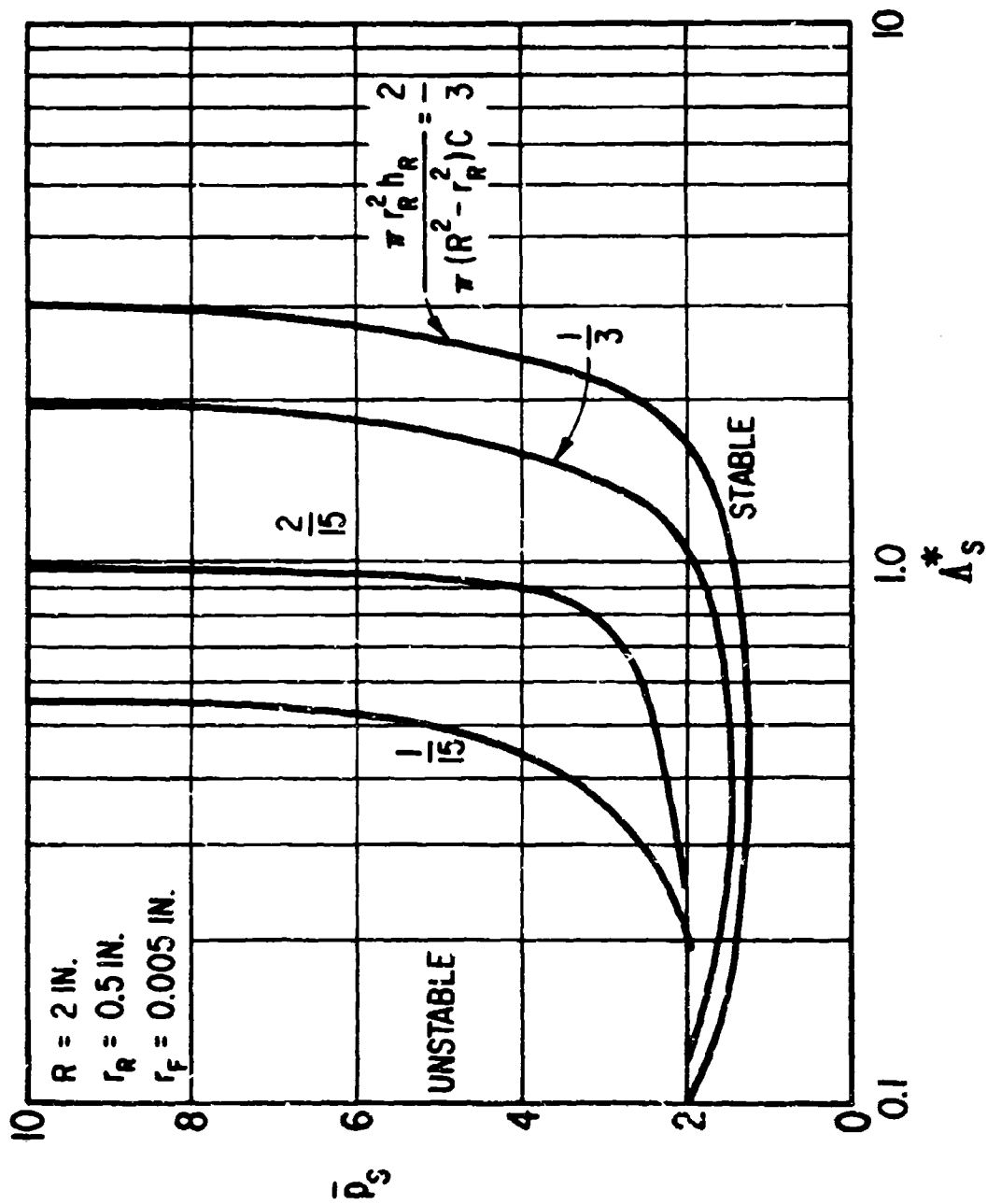


Fig. 12 Stability Map for Various Film-to-Pocket Volume Ratio



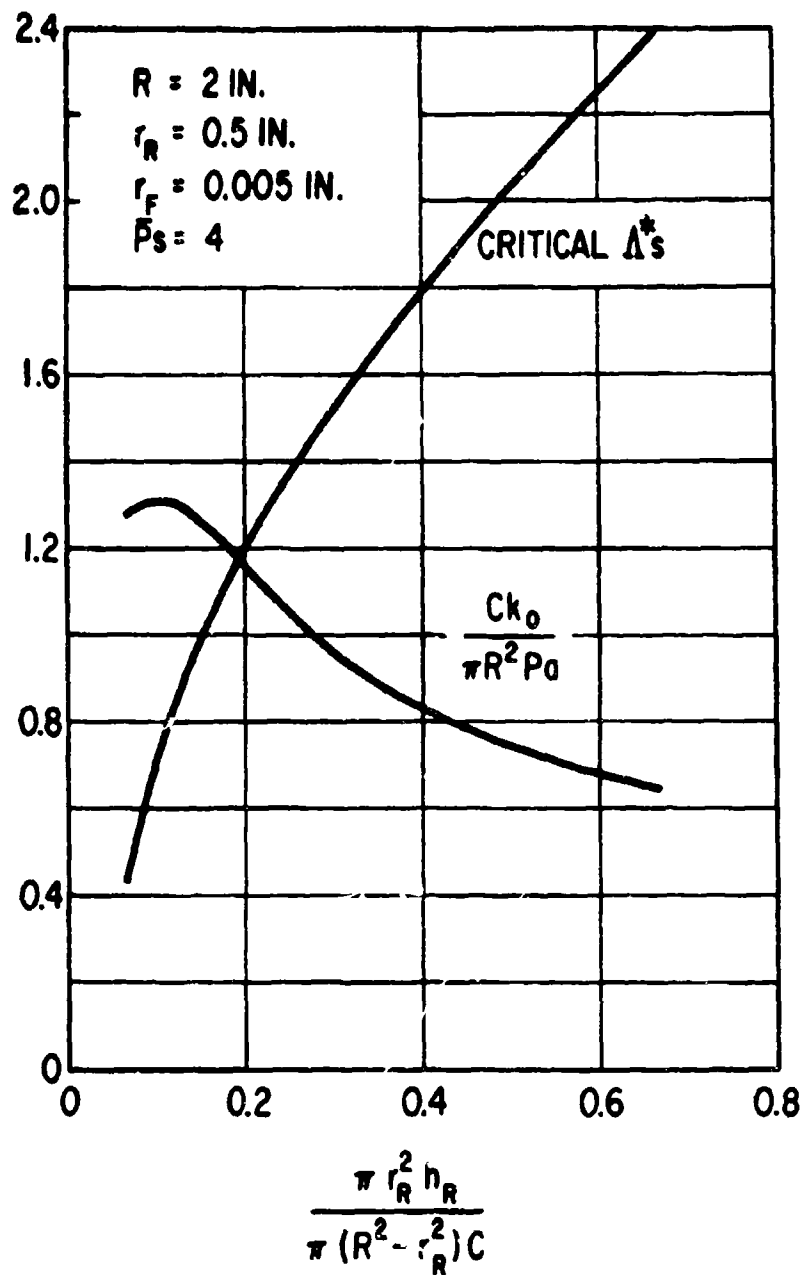


Fig. 13 Static Stiffness versus Film-to-Pocket Volume Ratio at the Respective Critical  $\Delta_s^*$

UNCLASSIFIED  
Security Classification

| DOCUMENT CONTROL DATA - R&D   |  |  |
|---|--|--|
| (Security classification of title, body of abstract and indexing annotation must be entered when the overall report is classified)  |  |  |
| 1. ORIGINATING ACTIVITY (Corporate author)<br>Mechanical Technology Incorporated<br>968 Albany-Shaker Road<br>Latham, New York 12110  |  | 2a. REPORT SECURITY CLASSIFICATION<br>Unclassified |
|   |  | 2b. GROUP  |
| 3. REPORT TITLE<br>Refined Solution of Pneumatic Hammer Instability of Inherently Compensated Hydrostatic Thrust Gas Bearings.  |  |  |
| 4. DESCRIPTIVE NOTES (Type of report and inclusive dates)<br>Technical Topical Report - March 1969  |  |  |
| 5. AUTHOR(S) (Last name, first name, initial)<br>Chiang, T.<br>Pan, Coda H. T.  |  |  |
| 6. REPORT DATE<br>March 1969  | 7a. TOTAL NO. OF PAGES<br>52   | 7b. NO. OF REFS<br>13                              |
| 8a. CONTRACT OR GRANT NO.<br>Nonr 3730(00)<br>b. PROJECT NO.<br>NR-062-317<br>c.<br>d.  | 9a. ORIGINATOR'S REPORT NUMBER(S)<br>MTI 69TR23<br>9b. OTHER REPORT NO(S) (Any other numbers that may be assigned this report) |  |
| 10. AVAILABILITY/LIMITATION NOTES<br>Distribution of this document is unlimited.  |  |  |
| 11. SUPPLEMENTARY NOTES   | 12. SPONSORING MILITARY ACTIVITY<br>U.S. Navy Department<br>Office of Naval Research   |  |
| 13. ABSTRACT<br>An externally-pressurized gas thrust bearing was analyzed for both static and dynamic characteristics. The bearing is fed through an inherently compensated restrictor into a shallow pocket. The analysis gave special attentions to the significance of the recent finding of restrictor flow (Ref: 4), the trade-off consideration between static stiffness and stability margin, and the effects of the pocket depth. ( ) |  |  |

DD FORM 1473  
1 JAN 64

Security Classification

UNCLASSIFIED

Security Classification

## DOCUMENT CONTROL DATA - R&amp;D

(Security classification of title, body of abstract and indexing annotation must be entered when the overall report is classified)

|   |  |  |                       |
|---|--|--|-----------------------|
| 1. ORIGINATING ACTIVITY (Corporate author)<br>Mechanical Technology Incorporated<br>968 Albany-Shaker Road<br>Latham, New York 12110  |  | 2a. REPORT SECURITY CLASSIFICATION<br>Unclassified                                       |                       |
|   |  | 2b. GROUP  |                       |
| 3. REPORT TITLE<br>Refined Solution of Pneumatic Hammer Instability of Inherently Compensated Hydrostatic Thrust Gas Bearings.  |  |  |                       |
| 4. DESCRIPTIVE NOTES (Type of report and inclusive dates)<br>Technical Topical Report - March 1969  |  |  |                       |
| 5. AUTHOR(S) (Last name, first name, initial)<br><br>Chiang, T.<br>Pan, Coda H. T.  |  |  |                       |
| 6. REPORT DATE<br>March 1969  |  | 7a. TOTAL NO. OF PAGES<br>52   | 7b. NO. OF REFS<br>13 |
| 8a. CONTRACT OR GRANT NO.<br>Nonr 3730(00)  |  | 8a. ORIGINATOR'S REPORT NUMBER(S)<br>MTI 69TR23  |                       |
| b. PROJECT NO.<br>NR-062-317  |  |  |                       |
| c.  |  | 8b. OTHER REPORT NO(S) (Any other numbers that may be assigned this report)              |                       |
| d.  |  |  |                       |
| 10. AVAILABILITY/LIMITATION NOTICES<br><br>Distribution of this document is unlimited.  |  |  |                       |
| 11. SUPPLEMENTARY NOTES   |  | 12. SPONSORING MILITARY ACTIVITY<br><br>U.S. Navy Department<br>Office of Naval Research |                       |
| 13. ABSTRACT<br><br>An externally-pressurized gas thrust bearing was analyzed for both static and dynamic characteristics. The bearing is fed through an inherently compensated restrictor into a shallow pocket. The analysis gave special attentions to the significance of the recent finding of restrictor flow, (Ref. 4), the trade-off consideration between static stiffness and stability margin, and the effects of the pocket depth ( ) ← |  |  |                       |

DD FORM 1473  
1 JAN 60

Security Classification